DESIGN AND CONSTRUCTION OF A RADIAL VELOCITY SPECTROMETER

by

JAMES RICHARD STILBORN

B.Sc., University of Manitoba, 1968

A THESIS SUBMITTED IN PARTIAL FULFILLMENT

OF THE REQUIREMENTS OF THE DEGREE OF

MASTER OF SCIENCE

in the Department

of

Physics

We accept this thesis as conforming

to the required standard

[redacted]

Accepted by the Faculty of Graduate Studies

on November 5, 1970 by [redacted] Dean of Faculty

UNIVERSITY OF VICTORIA

OCTOBER 1970

Supervisor: Dr. F.D.A. Hartwick

ABSTRACT

The design, construction, and operation of a photoelectric radial velocity spectrometer, based on the principles of an instrument described by R.F. Griffin (1967) is presented. Preliminary results of fourteen stars, observed at the 48-inch telescope of the Dominion Astrophysical Observatory, demonstrate that the instrument is useful to at least 8th magnitude over the spectral range G0 to M3 with a standard deviation of 2.8 km./sec. from the velocities of the General Catalogue of Stellar Radial Velocities of Wilson (1953).

Suggestions are given for further modifications to increase the accuracy and sensitivity of the spectrometer.

[redacted]

ACKNOWLEDGEMENTS

The writer wishes to thank his supervisor, Dr. F.D.A. Hartwick, for his assistance and enthusiastic encouragement.

This project would not have been possible without the use of the excellent facilities of the Dominion Astrophysical Observatory. The writer is grateful to the Director, Dr. K.O. Wright, for his permission to use the facilities. Much assistance was given by several staff members of the Observatory. Thanks are extended to Dr. E.H. Richardson for his help in designing the optical system, to Mr. R. Dancey for the cutting of the optical components, to Dr. J.B. Hutchings for his assistance during observing runs, and to Mr. R.N. Langton of the University of Victoria Physics Shop for his advice in metal machining procedures. The writer is especially indebted to Mr. J.M. Fletcher who spent many hours helping to make the instrument operational.

Financial support from the University of Victoria, in the form of a University of Victoria Graduate Fellowship, is gratefully acknowledged.

TABLE OF CONTENTS

LIST OF TABLES

LIST OF FIGURES

LIST OF SYMBOLS

Symbol	Definition
λ_o	Zero-velocity wavelength
λ	Wavelength
μ	Micron (10^{-6} meter)
σ	Standard deviation
Å	Ångstrom (10^{-10} meter)
c	Velocity of light
in.	Inch
mm.	Millimeter
cm.	Centimeter
km.	Kilometer
sec.	Second
V	Radial velocity
p.m.	Photomultiplier

CHAPTER 1

INTRODUCTION

The velocity of a star may be resolved into components, one of them being coincident with the vector from the Sun to the star. This component is called the radial velocity, and manifests itself as a Doppler shift in the stellar radiation. It is recorded in km./sec. and is taken as positive (+) if the velocity is away from the Sun, and negative (-) if it is toward the Sun. Radial velocities of stars in the neighbourhood of the Sun vary typically between -30 km./sec. and +30 km./sec. The orbital and rotational motions of the Earth relative to the Sun are responsible for a contribution of up to $\pm$ 29.9 km./sec. This contribution must be subtracted from the observed velocity to obtain the radial velocity of the star.

In a brief history of radial velocity measurements published by R.M. Petrie (1962), it is noted that in 1862 Huggins and Miller realized that a significant Doppler shift should be observable in the lines of stellar spectra, and the first but unsuccessful attempt at measurement was made by Huggins in 1866. Many similar experiments followed, in which stellar lines and lines of a laboratory emission source were viewed directly with the human eye. After a period of very limited success, the visual method was rendered obsolete at the turn of the century by the

introduction of the photographic recording of stellar spectra. The measurement of stellar spectrograms has since become a highly refined technique in the determination of stellar radial velocities.

A deviation from this technique was employed by R.F. Griffin (1967), and the description of his device, known as the Photoelectric Radial Velocity Spectrometer, inspired a feasibility study and formed the design basis of the instrument to be described in the following text.

CHAPTER 2

PRINCIPLE OF THE RADIAL VELOCITY SPECTROMETER

2.1 The Doppler shift and stellar spectra.

The principle of the dependence of the observed wavelength of light on the relative motion of source and observer was announced by Christian Doppler in 1842. In the classical form the dependence is given by the expression:

$$\frac{\lambda - \lambda_o}{\lambda_o} = \frac{\Delta\lambda}{\lambda_o} = \frac{V}{c}$$

Information concerning the source velocity will therefore be inherent in the light reaching the observer, and this velocity, as the radial velocity shall hereafter be called, may be calculated providing that certain features of known zero-velocity wavelength can be identified in the source spectrum. The absorption lines of stellar spectra are the information carriers in the case of stellar Doppler shifts.

2.2 The coincidence principle.

The visual radiation of a star is conventionally recorded in dispersed form as a spectrogram on a photographic plate. The reciprocal dispersion, specified in Å/mm. of plate, will depend on the design of the spectrograph. During the exposure by the stellar light, emission lines from a zero-velocity source, conventionally an iron arc, are recorded

above and below the band of stellar spectrum, providing zero-velocity reference lines. The developed spectrogram is of course a negative with the absorption lines appearing as lesser exposed gaps in the darker continuum.

If the developed spectrogram were to be placed at the focal surface of the spectrograph in precisely the same position as when the exposure was being made, a minimum amount of light would pass through the plate since light from the continuum would coincide with the exposed emulsion. It is assumed that the spectrograph remains stable and that the radial velocity does not change between exposure and reinsertion of the spectrogram. If the plate were then to be moved slowly either way parallel to the direction of dispersion, the continuum radiation would begin to fall on the many clear lines of the spectrogram and the amount of transmitted light would rise. In the case of stars of spectral type in the range F to M, the numbers and widths of lines are such that a strong attenuation of the light will occur at only one position of the plate. Many sub-coincidences will occur, but will be far less conspicuous than when all lines coincide.

The amount of attenuation by the spectrogram may be thought of as a cross-correlation function of the spectrogram and incident light of the stellar spectrum. If $F(\lambda)$ is the opacity of the plate as a function of wavelength, and $S(\lambda_1)$ is the wavelength distribution of the incoming starlight, and $P(\lambda - \lambda_1)$ is the instrumental profile of the

spectrograph, the attenuation as a function of plate position is given by the double convolution:

$$A(x)=\int_a^b F(\lambda-x)\left[\int_{-\infty}^{\infty} S(\lambda_1)P(\lambda-\lambda_1)d\lambda_1\right]dx$$

Providing that $F(\lambda)$ and $\int S(\lambda_1)P(\lambda-\lambda_1)d\lambda_1$ are sufficiently similar functions, $A(x)$ will be a maximum at $x=0$.

Similarly, the emission lines of the zero-velocity comparison source will cause a minimum, or dip as it will now be called, when the dark lines of the comparison spectrogram have been brought into register. The comparison source coincidence therefore enables one to determine the zero-velocity position of the plate.

The displacement of the mask, as the spectrogram-bearing plate will now be called, must then be converted into the stellar radial velocity from the Doppler relation. As mentioned, the reciprocal dispersion of the spectrograph is given in Å/mm. To illustrate the reduction procedure a simple example is presented. Suppose that it is found by the above technique that the coincidence of a line at 4500 Å occurs when the mask is $10\mu=10^{-2}$mm. from the zero-velocity position, in the direction of increasing wavelength. If the reciprocal dispersion of the spectrograph is 4 Å/mm., the line has been Doppler shifted by 4 Å/mm. $\times 10^{-2}$mm.$=$ .04 Å. Assuming the velocity of light to be $c=3.0\times10^5$km./sec., the radial velocity is calculated to be $V=c\,\Delta\lambda/\lambda_\circ=+2.67$ km./sec.

To facilitate calculations, the velocity corresponding to a displacement of 1.0 mm. is tabulated over the relevant range of wavelengths. It is known as the rVs factor, and is 267 km./sec./mm. at 4500 Å for the spectrograph in the example.

The spectral range of the mask in the instrument to be described is about 400 Å, and so different lines of a non-zero velocity source will coincide at slightly different displacements, assuming that the reciprocal dispersion is constant. This effect will be discussed when the specific masks used in the instrument are described.

2.3 Comparison with the photographic technique.

The measurement of stellar radial velocities by photography of spectra is a well-established technique. The justification for constructing a radial velocity spectrometer, henceforth referred to as the R.V.S., can best be illustrated by consideration of the relative merits of a single-channel detector, in this case the photomultiplier, versus those of a multi-channel detector, or the photographic plate.

In the case of the photographic plate, each recorded absorption line contains information of the source velocity. Extraction of the information requires that the position of each line be measured with a travelling microscope, or some similar device modified especially for the measurement of stellar plates. Lines of both stellar and iron spectra which are known to be reliable for radial velocity purposes

are listed along with the rVs factor in tables. To minimize random errors it is desirable to measure as many lines as possible, usually about 25 for a G or K type star, plus about 10 comparison lines. The method is reliable and can be used for all spectral types, but is time consuming. The exposure time for a 5th magnitude star on the same spectrograph as is used with the R.V.S. is typically from 40 to 60 minutes. Measurement of the plate and reduction of the results requires from 1 to 2 hours for an experienced operator.

The photoelectric technique utilizes a single-channel detector, the photomultiplier, and simultaneously measures as many lines as there are on the mask. In the preliminary trials of the instrument, both slow and rapid scanning techniques required about twenty minutes and eight minutes per star, respectively. In both cases the dips were recorded on graph paper and displacements were simply measured with a ruler, requiring about one-half hour per star.

In addition, the quantum efficiency of a photo-multiplier may be as high as 50 per cent; in other words, about one of every two incident photons produces a photo-event, whereas the emulsions of the type used in astronomical work have efficiencies as low as 0.1 or 0.2 per cent. If one were to include the superior efficiency of the photomultiplier along with the fact that it measures at least 200 lines simultaneously, an anomalously high gain in speed would be apparent. This is not the case however, owing to the fact that the photographic emulsion integrates all lines continuously,

whereas the photomultiplier is made to scan and records useful information in the region of the dip during only a small fraction of the scan time. Also, it is not realistic to compare the highest attainable efficiency of a photomultiplier with the poorest efficiency of a plate. In practice, the quantum efficiency of a photomultiplier is from ten to twenty times that of a photographic emulsion.

Although a line-by-line reduction of a spectrogram is very time consuming, it has the advantage of being selective as to the quality of the lines being measured, and the operator is able to reject unreliable or blended lines. Photoelectric scans yield an average displacement for over 200 lines, most of which vary greatly in quality from star to star.

A factor of merit useful in comparing the two techniques is the speed-accuracy product. At the present stage of refinement the R.V.S. performance is of roughly equal merit to the photographic method, but the writer estimates that a practical limit for such an instrument may be a gain of about 20 to 100 times, or an equal speed-accuracy product for photoelectric velocities of stars from three to five magnitudes fainter.

CHAPTER 3

SPECTROMETER COMPONENTS AND OPERATION

3.1 The mask.

The first mask produced was simply a solar spectrogram from an exposure of the sky. Scans were performed using the sky, which is about 4 magnitudes per square second of arc. Only a very shallow dip was recorded, probably on account of the high transmission of the spectrogram and the spillage of light above and below the exposed strip. Subsequently an artificial mask was produced by the device described in Appendix B. The image of a slit source was projected onto a standard 2-inch by 8-inch photographic plate, exposing it in positions corresponding to lines on the original sky plate. A contact print was made of this, producing a completely black mask with apertures corresponding to the lines. This substantially reduced the transmission and prevented spillage of light around the spectrum. The transmittance was determined by measuring the areas of all the lines on a microphotometer tracing. Table 3.1.1 is a listing of the characteristics of the mask used in the first seven velocity measurements. As the Sun is a star of spectral class G2 V, the first mask will be referred to as the G2 V mask.

Limits:	Red end - 4736.8 Å
	Blue end - 4360.7 Å
Range:	376.1 Å
Transmittance:	2.6 per cent
Number of stellar lines:	207
Number of comparison lines:	20
Line widths:	30μ to 120μ
Effective rVs factor:	156.5 km./sec./mm.

Table 3.1.1

Characteristics of the G2 V mask.

The rVs factor was calculated for a number of intervals along the mask. The average, or effective rVs factor for the plate was obtained by finding the center of transmission in a manner analogous to a center of gravity calculation. More specifically:

$$\bar{\lambda} = \frac{\Sigma(\text{line area}) \times (\text{wavelength})}{\Sigma(\text{line area})}$$

The summation extends over all lines. The result was 4544 Å at which the rVs factor is 156.5 km./sec./mm. The actual center of transmission during operation will depend upon the brightness distribution of the lines of the particular star being measured, and is not accounted for. As mentioned in Section 2.2, the rVs factor is not constant, and hence lines at different wavelengths will coincide at different mask positions whenever the source velocity is not zero. Let us suppose that coincidence is achieved at the center of

transmission where rVs = 156.5. At the red end, rVs = 149.5, and at the blue end, rVs = 163.3. Let us also assume that the radial velocity of the star is 156.5 km./sec. This will result in a mismatch of about 7 km./sec. at either end of the mask. However, a typical half-width of the dip is about 50 km./sec., and so the mismatch does not degrade the dip appreciably even at this high velocity.

The stellar lines will effect a minimum in signal at coincidence, but the comparison lines will cause a maximum since the comparison source has an emission-line spectrum, and the artificial mask has apertures rather than dark lines as on the sky spectrogram.

All comparison lines were transferred from the sky plate, but only those solar lines having widths from 30μ to 120μ were used. Results indicated that accuracy and spectral type had no correlation over the range G0 to M3.

An improved mask corresponding to Arcturus, a K2 III star, was used in obtaining the seven remaining velocities. The characteristics are listed in Table 3.1.2.

Limits:	Red end - 4736.8 Å
	Blue end - 4365.9 Å
Range:	370.9 Å
Transmittance:	5.8 per cent
Number of stellar lines:	246
Number of comparison lines:	15
Line widths:	40μ to 120μ
Effective rVs factor:	158.7 km./sec./mm.

Table 3.1.2

Characteristics of the K2 III mask.

3.2 Optical system.

A one-half scale diagram of the optical components is given in Figure 3.2.1. In order to determine the optimum spacing, the lenses were mounted on an adjustable optical test bench and were moved until a good focus was achieved. The f/7 beam of the spectrograph was focussed into an image of the gratings 17.5 mm. on edge. This was acceptable, as the photocathode diameter was 23 mm.

To facilitate mounting, the primary lens was cut leaving a 2-inch by 8-inch section. No light loss resulted since the spectrograph beam was less than 3 mm. high at the focal plane, immediately behind which the primary lens was mounted.

The converging beam had to be diverted 90° into the R.V.S. optics because the scanning direction was parallel

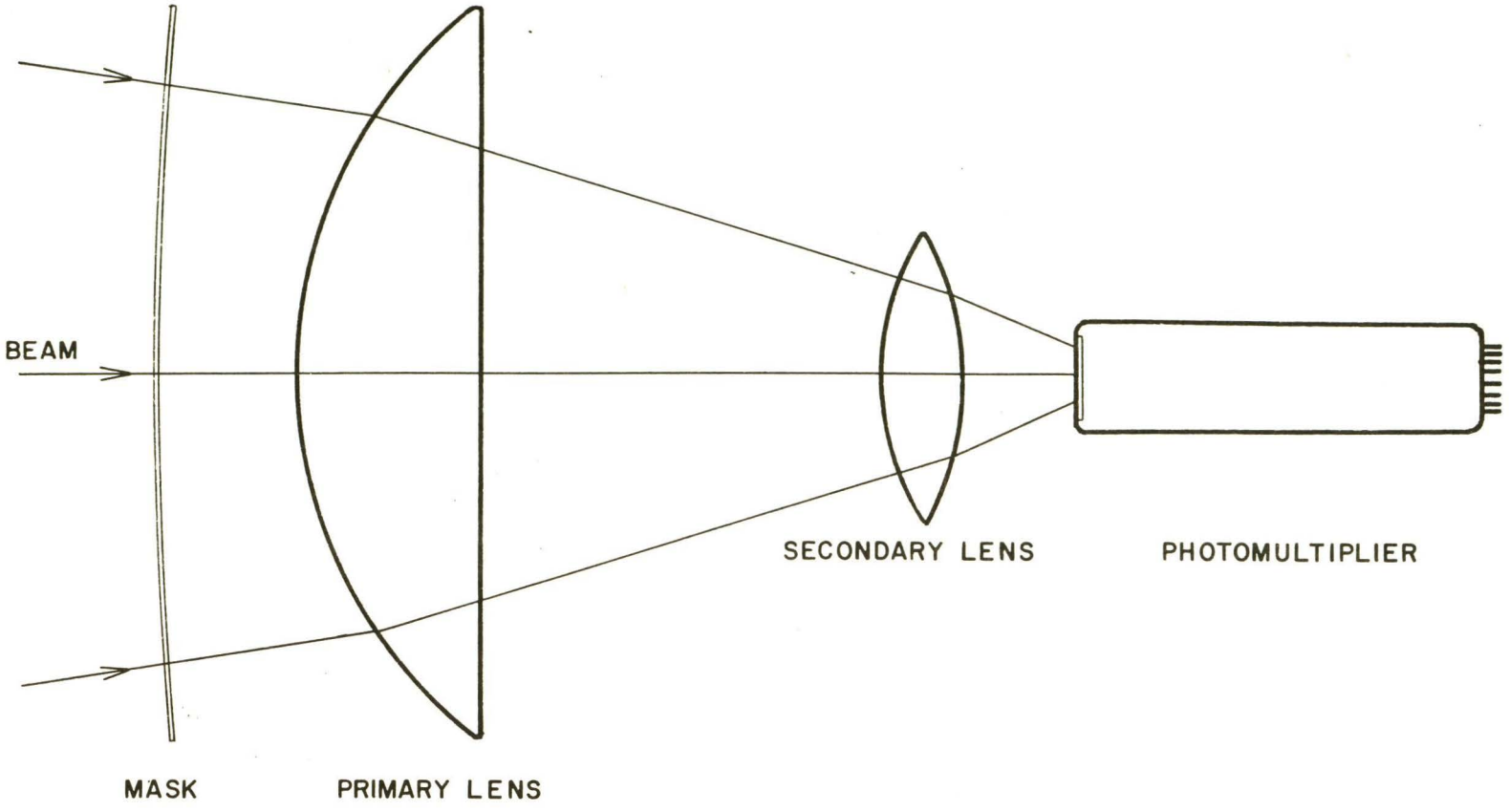

Figure 3.2.1

Optical components, one-half scale

to the original beam. For this, a 2-inch by 15-inch mirror was used as in Figure 3.2.2. The mirror was cut from a piece of 3/4-inch thick plate glass and was aluminized without any optical figuring of the surface. The plate glass was deemed to be sufficiently flat to divert the beam with a negligible degradation of the focus. The appearance of a double comparison dip, noticeable in Figure 4.1.2, raised suspicions as to the quality of the reflecting surface. Subsequent tests by J.M. Fletcher showed the mirror to be of acceptable flatness over only two-thirds of the length of the surface.

The mirror holder is provided with three adjustable supporting screws for alignment in height , and with a rotatable base for alignment in azimuth. The holder is situated in the beam between the grating and camera mirror. The optics of the image slicer arrange the incoming starlight into horizontal slices, and the slice coincident with the mirror holder is missing, the slices having been aligned so as not to allow any obstruction by the holder. The operation of the image slicer is described in a publication of E.H. Richardson (1968).

3.3 Photomultiplier and electronics.

Figures 3.3.1 and 3.3.2 are flow diagrams of the R.V.S. electronics for the slow scan and rapid scan modes, respectively.

In the slow scan mode the output of the 9524S photomultiplier is displayed on a Honeywell-Brown strip-

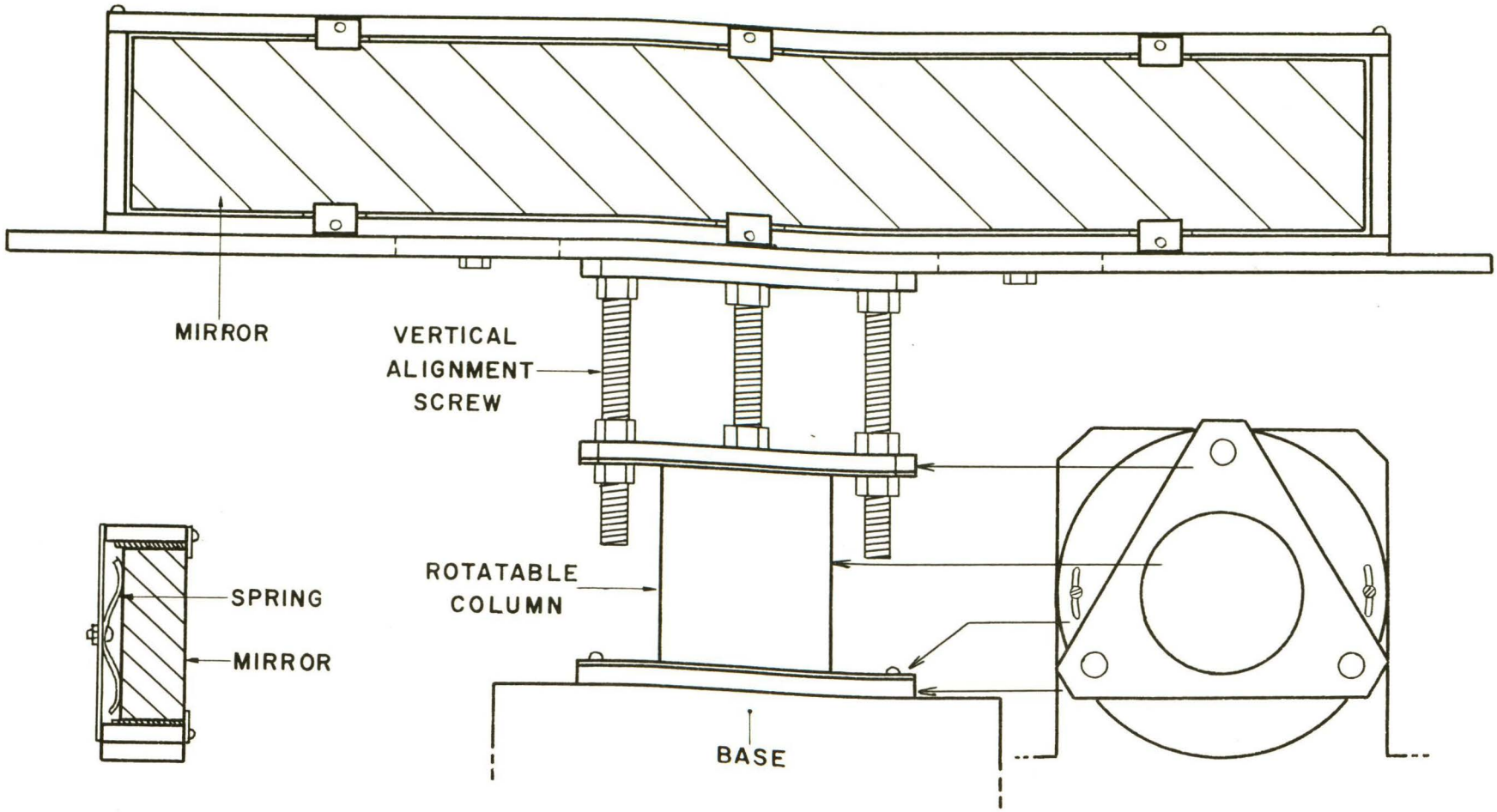

Figure 3.2.2

Mirror and holder

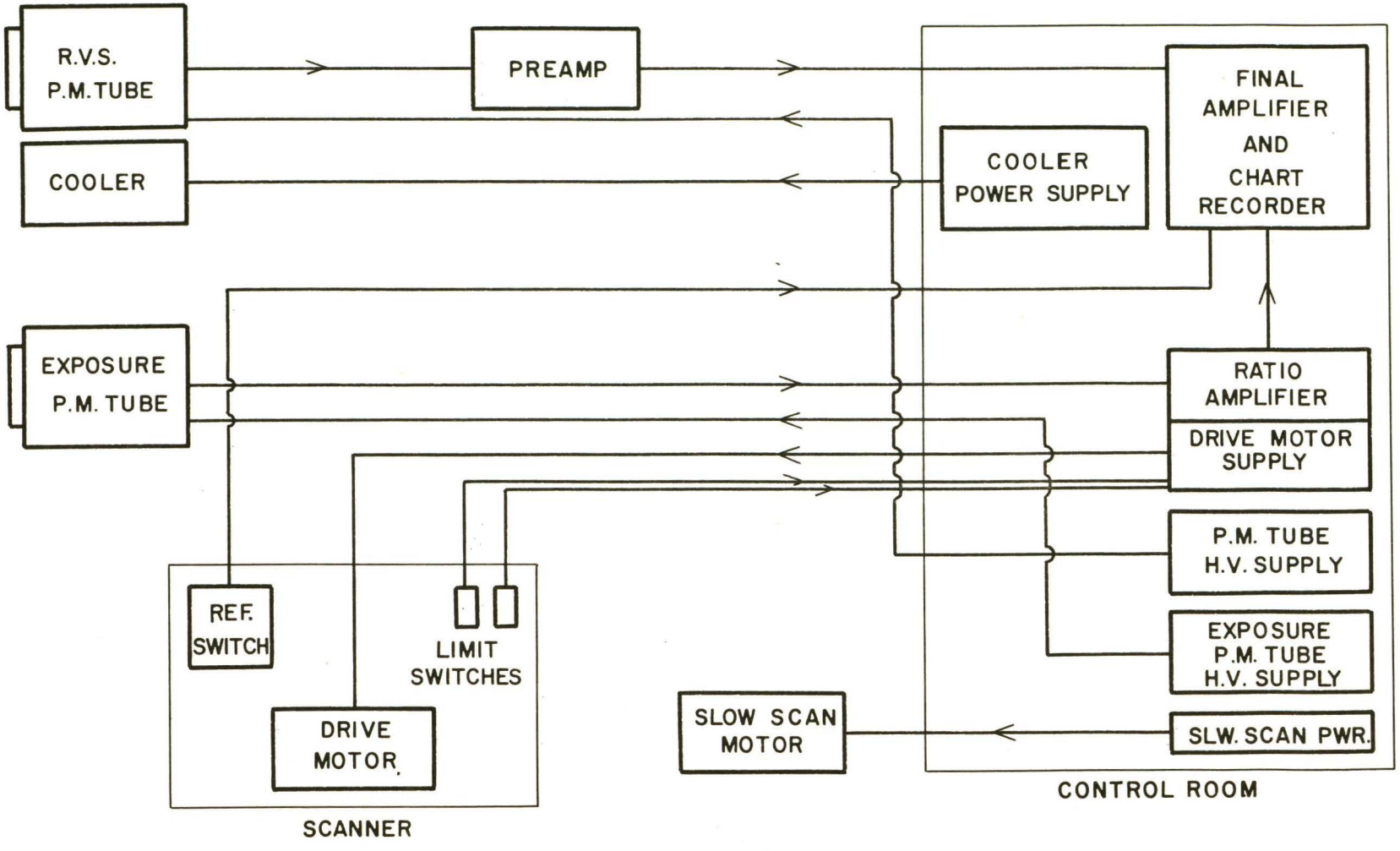

Figure 3.3.1

Electrical system for the slow scanning mode

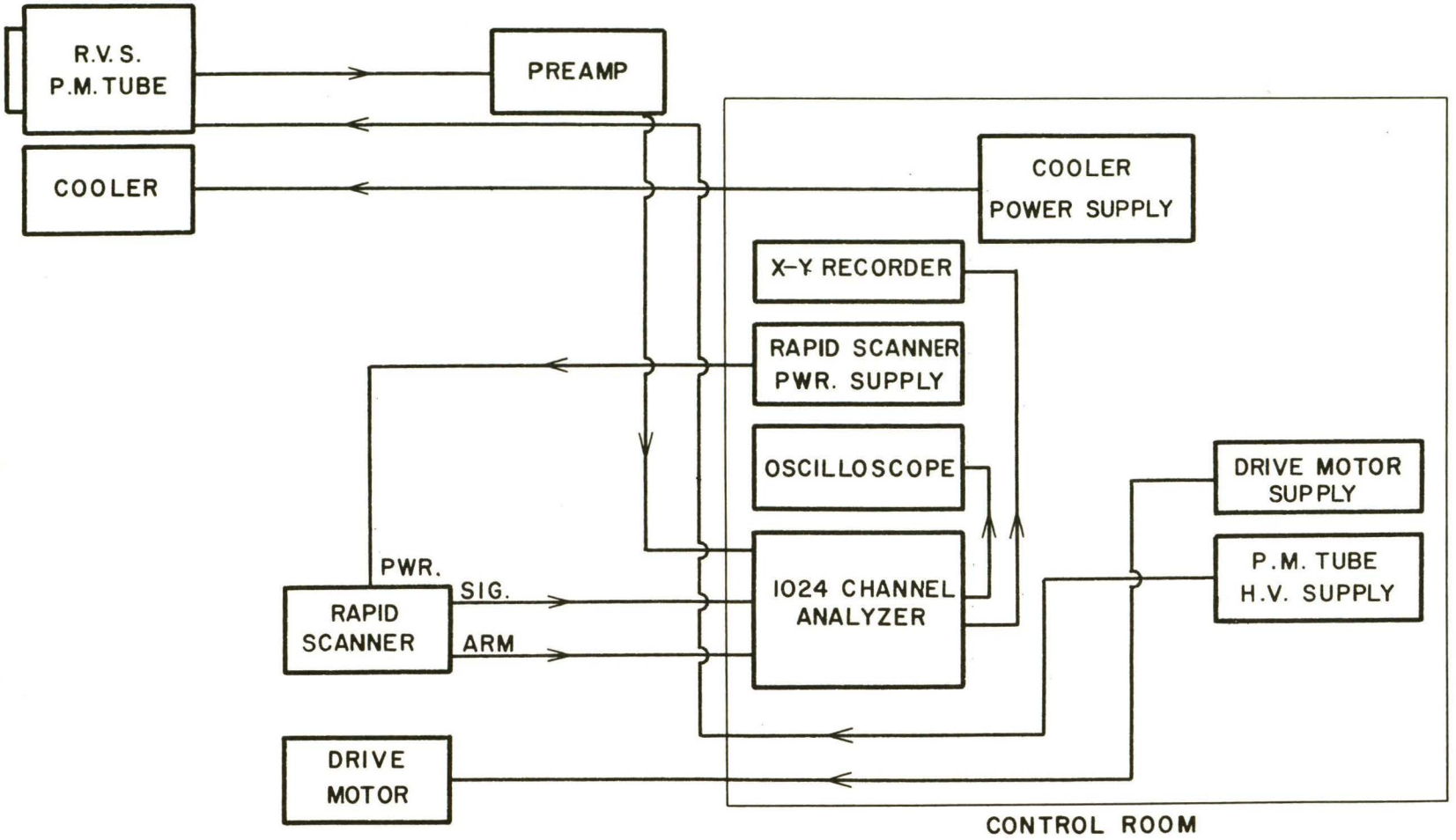

Figure 3.3.2

Electrical system for the rapid scanning mode

chart recorder. In addition, output from the exposure meter, which monitors about 5 per cent of the incoming starlight extracted by a beam splitter just behind the slit, is fed to the recorder and furnishes a reference voltage. Thus the recorded output is a ratio between the incoming light and the spectrometer output. This technique, developed by J.B. Hutchings, reduces fluctuations seen occurring in the trace as a result of changes in apparent star brightness caused by sky haze and unsteadiness of the stellar image on the slit. The trace will remain steady over a range of brightness of about 2 times. When the coincidence is achieved, the ratio is of course changed and a dip is recorded. The ratio technique is not used when scanning the comparison lines since atmospheric effects are absent.

The photomultiplier signal is initially amplified by a small preamp close to the R.V.S. in order to minimize interference from stray pickup before final amplification. It is seen in Figure 3.3.3 as a grey box to the rear of the spectrometer. Amplification, zero point adjustment, and time constant are all controlled by the three knobs on top of the preamp. The settings used are described in Section 3.8.

The photomultiplier is cooled to -20° C. by a thermoelectric cold plate cooler. The heat is transferred to circulating water in a cooling jacket.

The scanning platform is moved by a precision screw

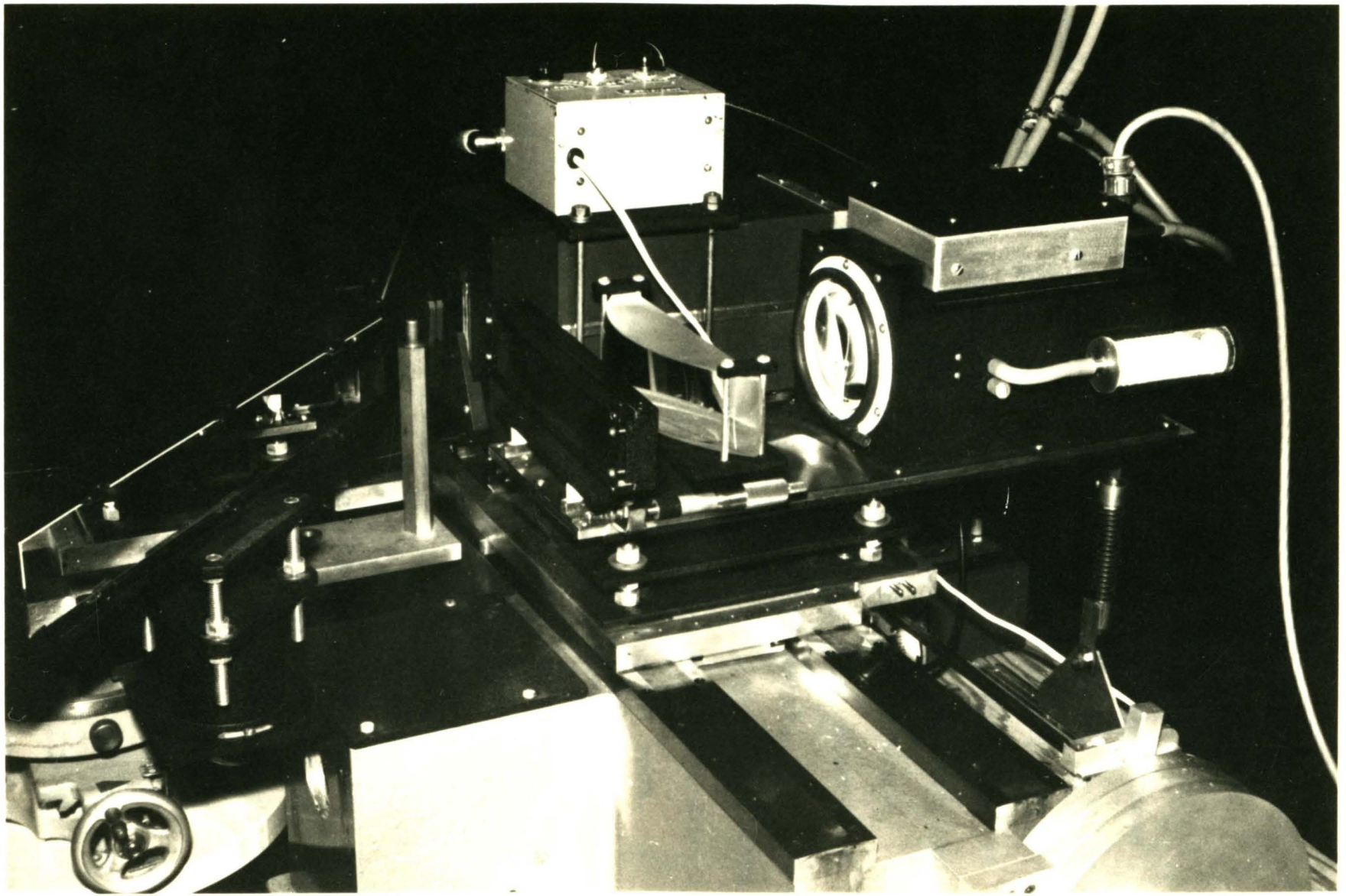

Figure 3.3.3

Spectrometer and scanner.

geared to a variable-speed drive motor. A microswitch is momentarily closed at each revolution of the screw by a small stud projecting from a wheel at one end of the screw. Since the pitch of the screw is 1.0 mm., the switch closes every 156.5 km./sec. and shorts the chart recorder, producing a reference grid of downward spikes against which the dips can be measured. Shorting microswitches are also placed at both ends of travel of the scanner platform to turn off the drive motor whenever the platform is in danger of being driven against the ends of the screw. The small motor used in the Hartmann focus test, to be described later, is controlled from a power supply in the control room. All controls, with the exception of the preamp and cooling power supply, are mounted together in vertical racks in the control room.

The slow scanning apparatus and all of the associated electronics were designed and built by J.B. Hutchings and W.G. Smythe of the Dominion Astrophysical Observatory.

In the rapid scanning mode the output is again preamplified and is integrated by a 1024-channel analyzer. The signal is preamplified with negligible time constant at the spectrometer. Final amplification and time constant are adjusted at the analyzer. In this mode the mask is stationary and the spectrum is diplaced 1.2 mm. along the mask every 0.25 sec. by refraction through a rotating glass plate. The plate and rotating mounting are shown in Figure 3.3.4, in position behind the slit. A series of slits on the periphery of the large mounting disc forms the channel advance system

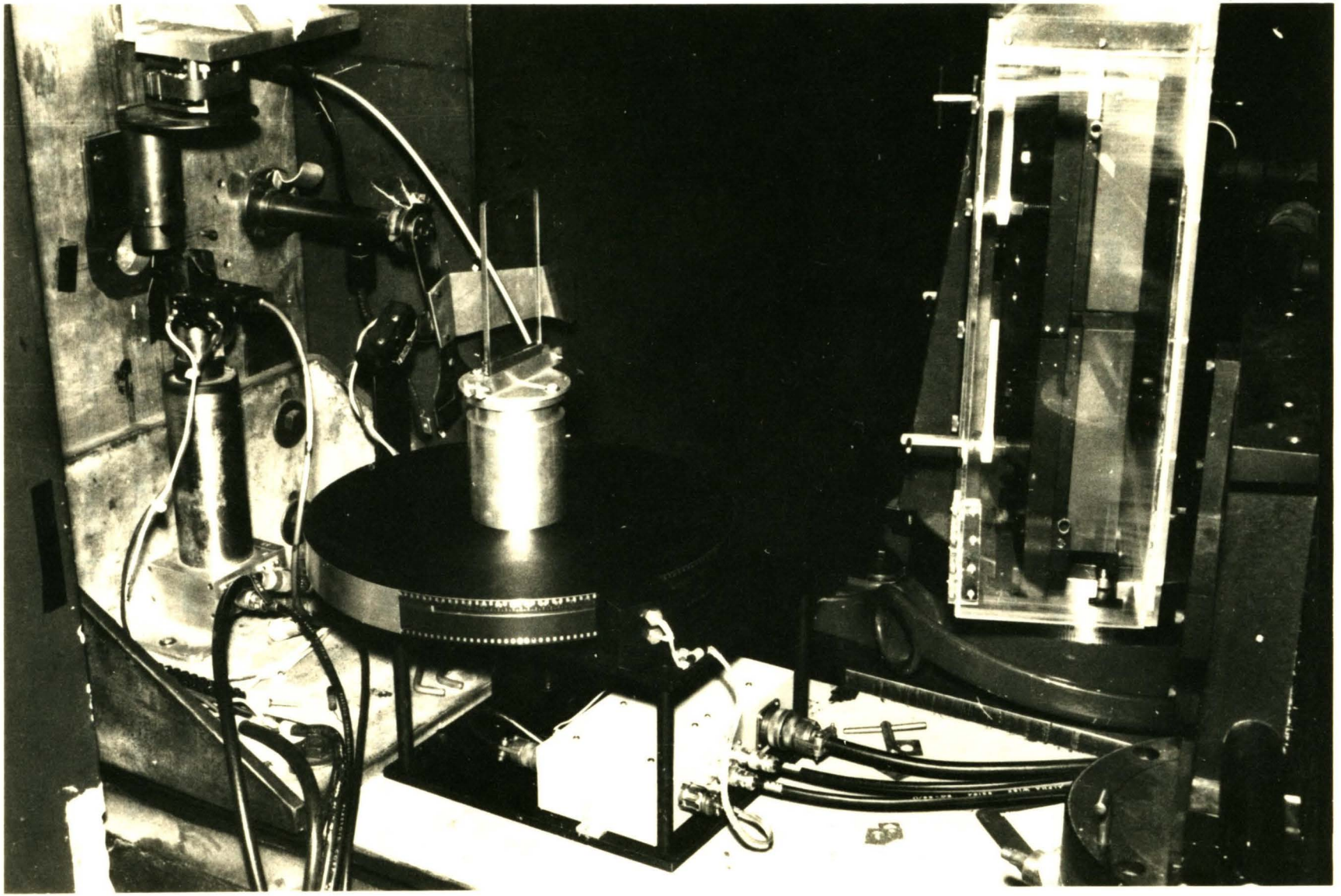

Figure 3.3.4

Beam entrance, rapid scanner, and mosaic grating.

for the analyzer. A photodiode mounted on the outside receives light from a source inside the slits, and the pulsed output is fed to a Schmidt trigger and then to the analyzer. A second photodiode supplies an arming pulse for the analyzer at the commencement of each scan. The light is scanned twice by the glass per revolution of the disc; thus, two sets of slits are provided so that both scans can be recorded.

3.4 Scanning mechanisms.

The stationary base of the entire slow scanning assembly is visible as the large bulk at the bottom foreground of Figure 3.3.3. The two wide rails on which the platform slides are clearly visible, in addition to the platform itself and the spectrometer baseplate. The screw is located behind the stationary base. A diagram of the complete assembly is given in Figure 3.4.1. Figure 3.4.2 shows the dimensions of the baseplate which is bolted to the moving platform. The baseplate is adjustable in height, and the upper plate upon which all R.V.S. components are mounted is adjustable in the direction of focus.

The drive motor, not visible in the figure, is operated from the control room. The screw works against a heavy lead weight which, by a cable and pulley system, applies force on the scanner platform in the direction of the blue end of the spectrum, or into the page. The three large discs visible in the lower right corner are positioned

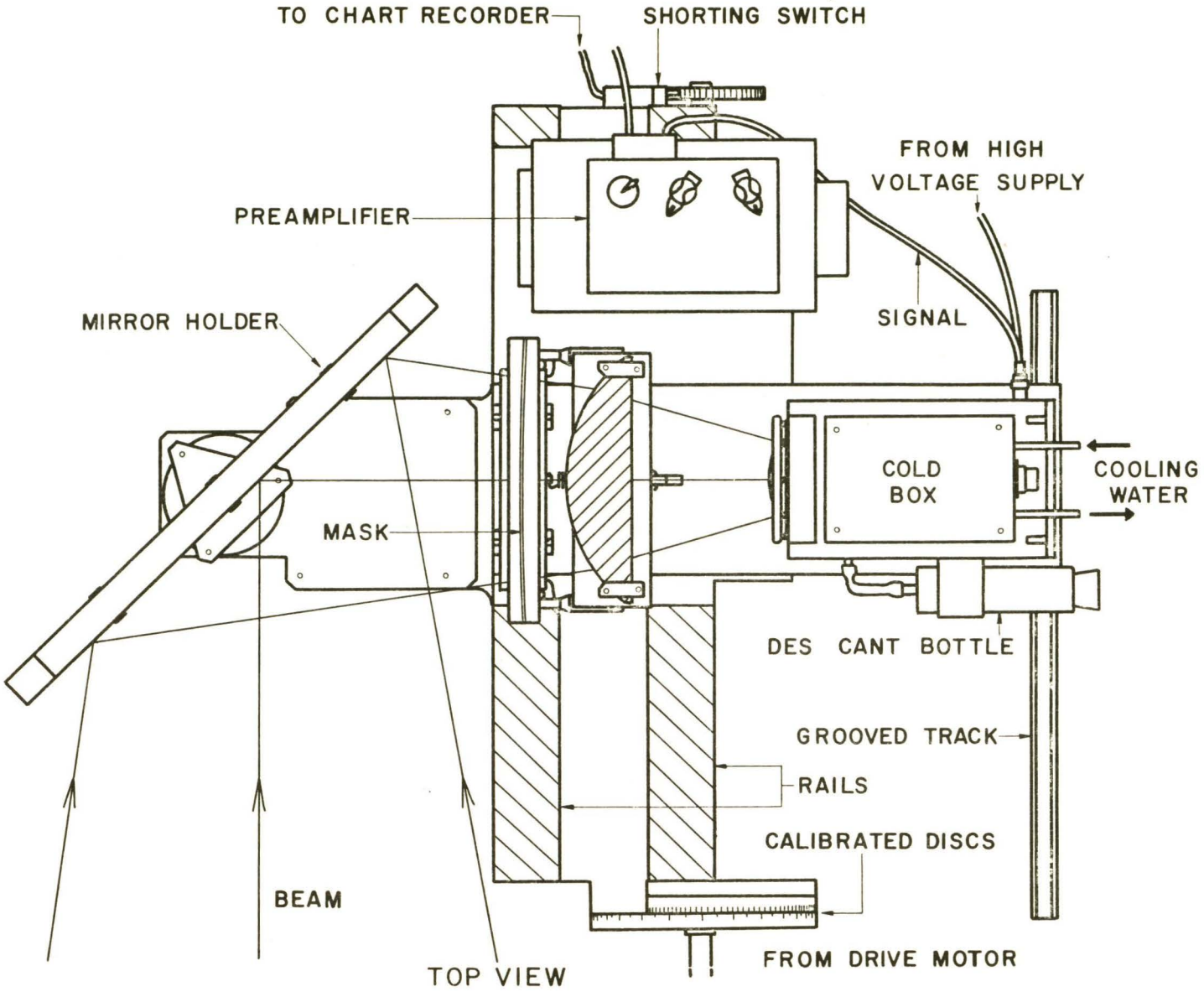

Figure 3.4.1
Integrated instrument on the slow scanner

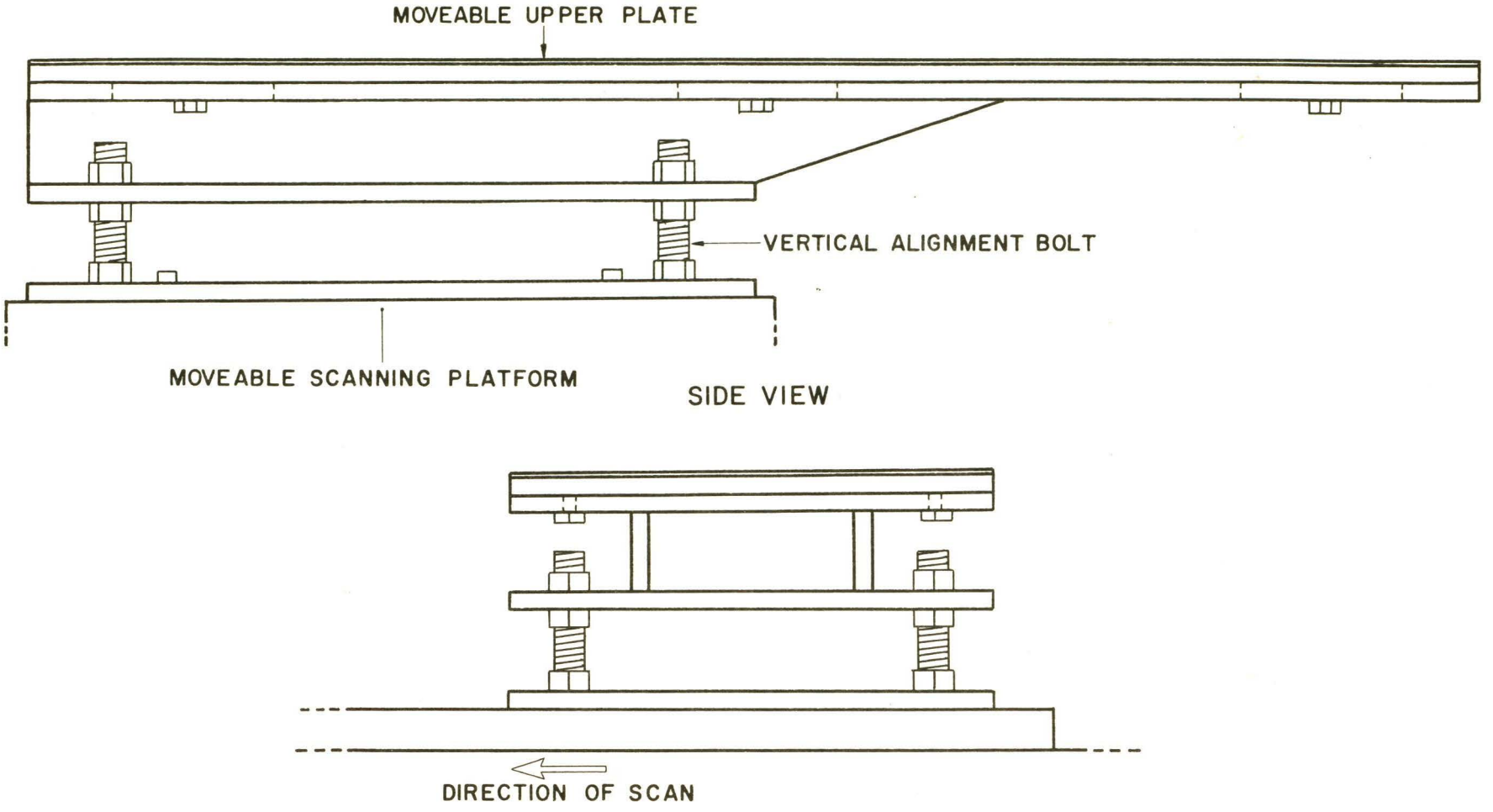

Figure 3.4.2

Baseplate, one-half scale

concentrically on the shaft of the screw. The scale engraved on the discs is used to position the platform roughly during alignment.

The mirror holder is attached directly to the stationary base by four easily removed machine screws, since the mirror must be removed when the spectrograph is to be used for conventional photography.

Most of the mass was concentrated in the cold box. This caused the platform to rock on the rear rail. Applying more weight to the front of the machine caused the platform to bind on the oiled rails when scanning toward the blue. Instead of applying weight, an upward thrusting spring was installed beneath the rear of the baseplate. The spring follows the motion of the platform by means of two wheels that follow a grooved aluminum track.

The rapid scanner, designed by D.H. Andrews, W.G. Smythe, and J.M. Fletcher, is attached behind the slit as seen in Figure 3.3.4. The large plexiglass box to the right houses the mosaic grating. A diagrammatical representation of the rapid scanner is given in Figure 3.4.3. The motor rotates the refracting plate at one revolution per second, and each set of address slits covers 90° of the disc circumference; hence, each scan lasts 0.25 sec. The beam displacement is not a linear function of plate angle, a fact that must be taken into account when the data is to be reduced.

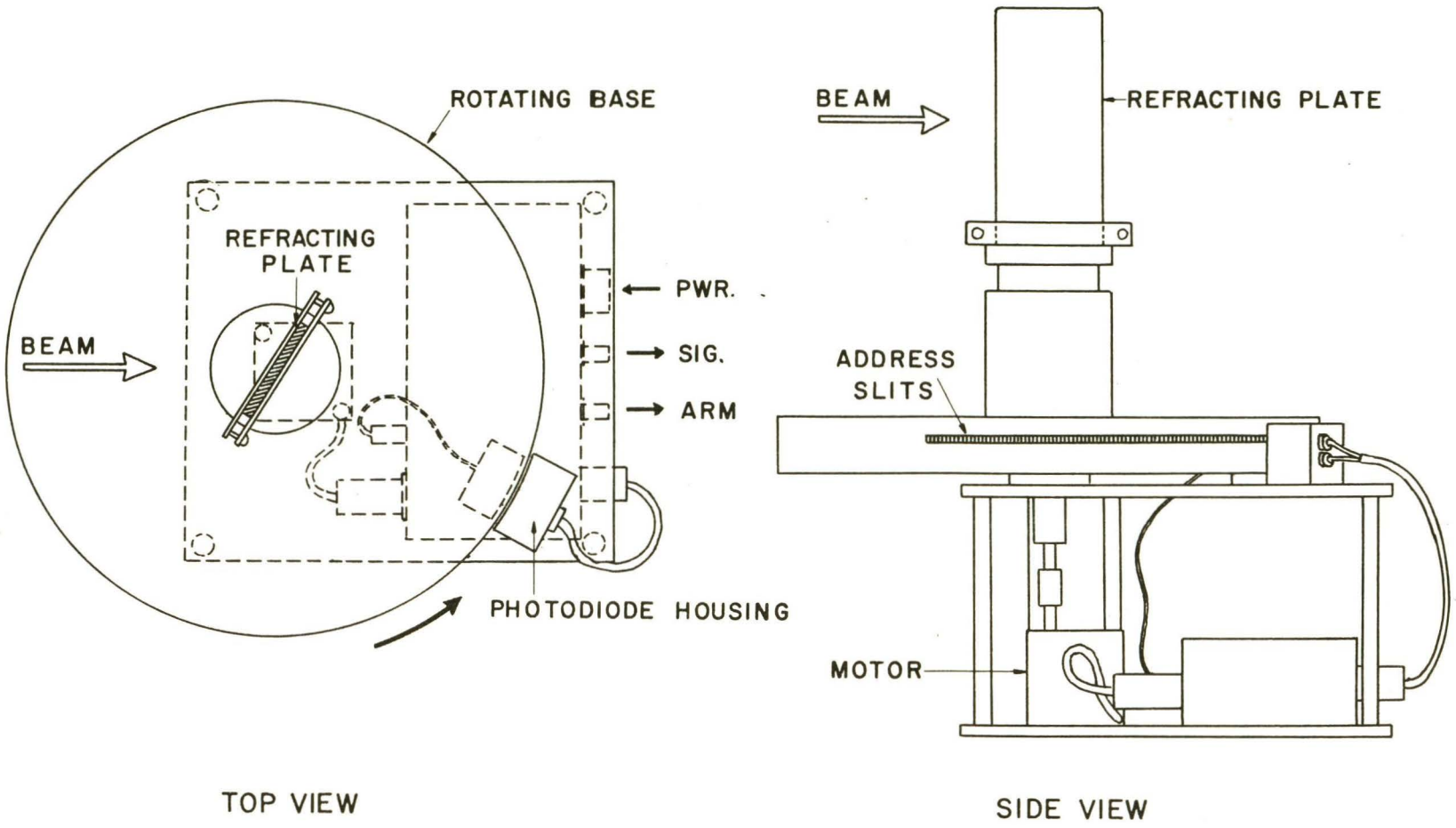

Figure 3.4.3

Rapid scanner, one-quarter scale

3.5 The maskholder.

The maskholder is shown in Figure 3.5.1 and Figure 3.5.2. It is adjustable in height and tilt by three support screws, and is also adjustable horizontally in the direction of focus. The focus adjustment is made by two micrometer screws so that each end of the mask may be focussed independently. The screws work against a compression spring, and the assembly is supported by two oiled teflon runners held snugly within brass flanges.

The mask is installed by first removing the front of the holder. The mask is centered by hand, the front is replaced, and then it is pressed firmly against the mask by four machine screws. Minor position adjustments are made by backing off the screws slightly and pressing the edge of the mask with a thumbnail or screwdriver.

The focal plane is not planar but is curved with a radius of 96 inches. Hence the two surfaces holding the mask had to be cut and ground to this radius. Because of this curvature, as soon as a scan is made to the left or right, the spectrum is no longer in focus. However, for a scan of 1 mm. in either direction, the defocussing over the 16 cm. of the mask used amounts to a harmless .008 mm.

3.6 Lens holder and photomultiplier cold box.

The primary lens holder is shown in Figure 3.6.1. The mounting is not adjustable. The lens is held fast to the lower rubber-padded plate by two rubber-padded retainers and four bolts.

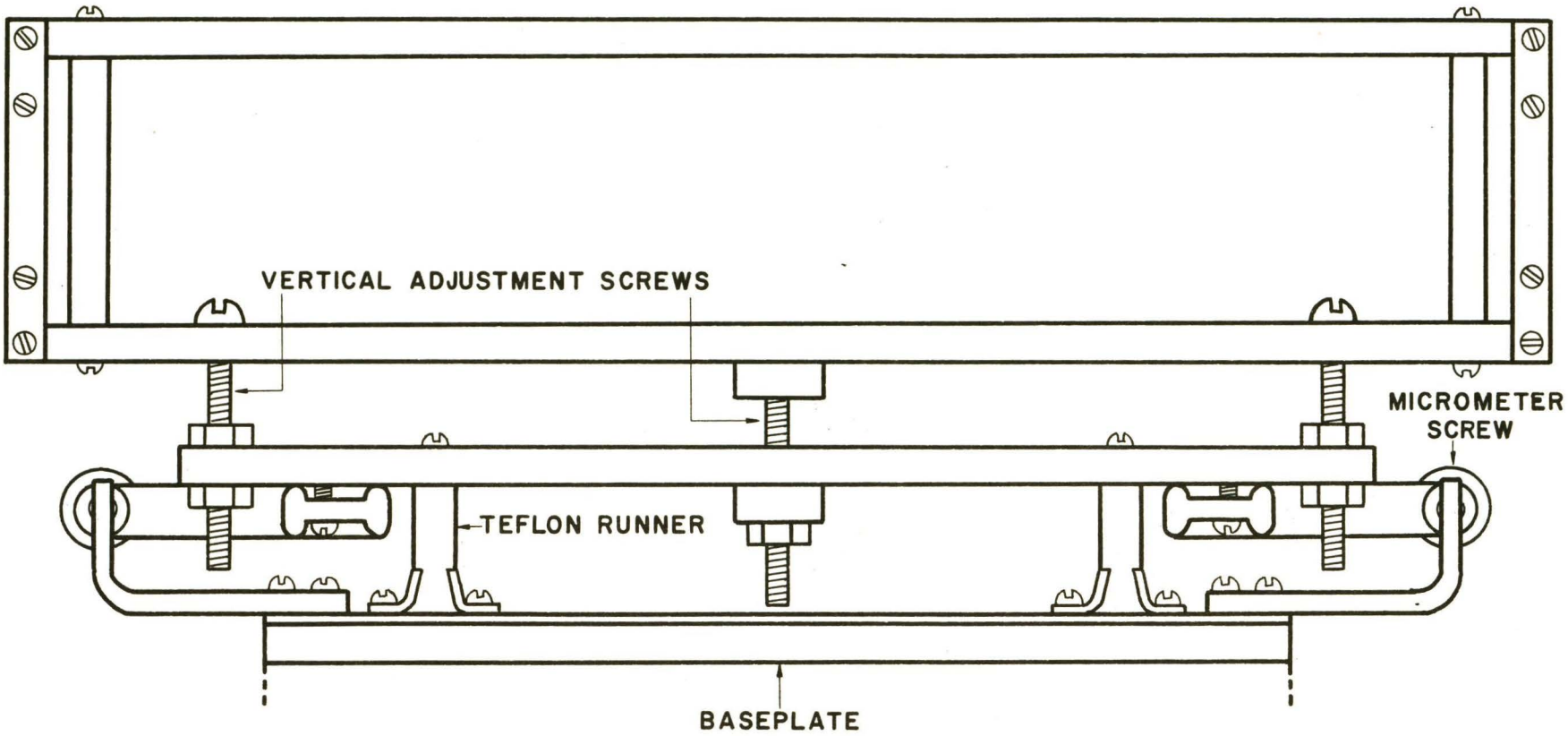

Figure 3.5.1

Maskholder, front view, full scale

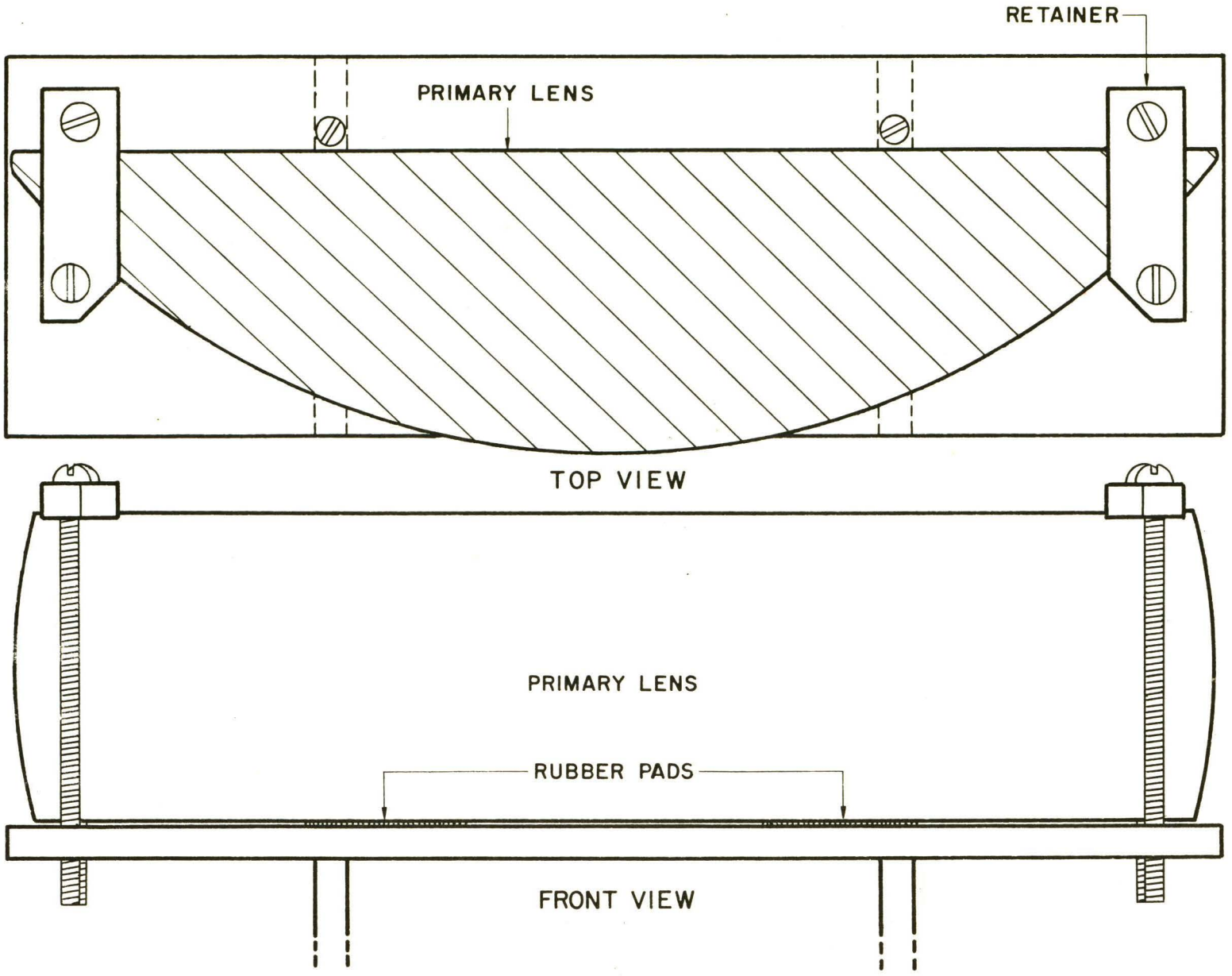

Figure 3.6.1

Primary lens holder, full scale

The refrigerated photomultiplier housing is illustrated in Figure 3.6.2 and Figure 3.6.3. The figures are self-explanatory, but several features are worthy of mention. The thermoelectric cooler is mounted on top with the cold element protruding into a rectangular hole cut in the top of the cylindrical inner housing. The photomultiplier immediately below is supported by only the socket, which is quite sufficient. It is shielded by a μ-metal sleeve at cathode potential to minimize effects from stray fields. Access to the voltage divider chain is gained through two removable hatches at the rear of the box. If the p.m. tube is to be inspected, the top of the box must be removed. The hatches are sealed with gaskets and the seal around the cooling element is rendered airtight with heavy grease. The secondary lens is thermally insulated from the cold chamber by a clear glass plate and rolled paper mounting. A ring of copper tubing with six small holes directed at the lens is installed so that warm air can be blown over the lens in the event of frosting. It was found to be an unnecessary feature.

While the inner housing is being cooled, the air pressure within is reduced. Humidity can be a source of noise due to leakage currents caused by high voltage, and so moist air has to be prevented from entering the housing during cooling. The solution of making the box completely airtight introduces sealing difficulties, and so an arrangement called a breathing desiccator is used. Any air entering the housing follows the low-resistance path

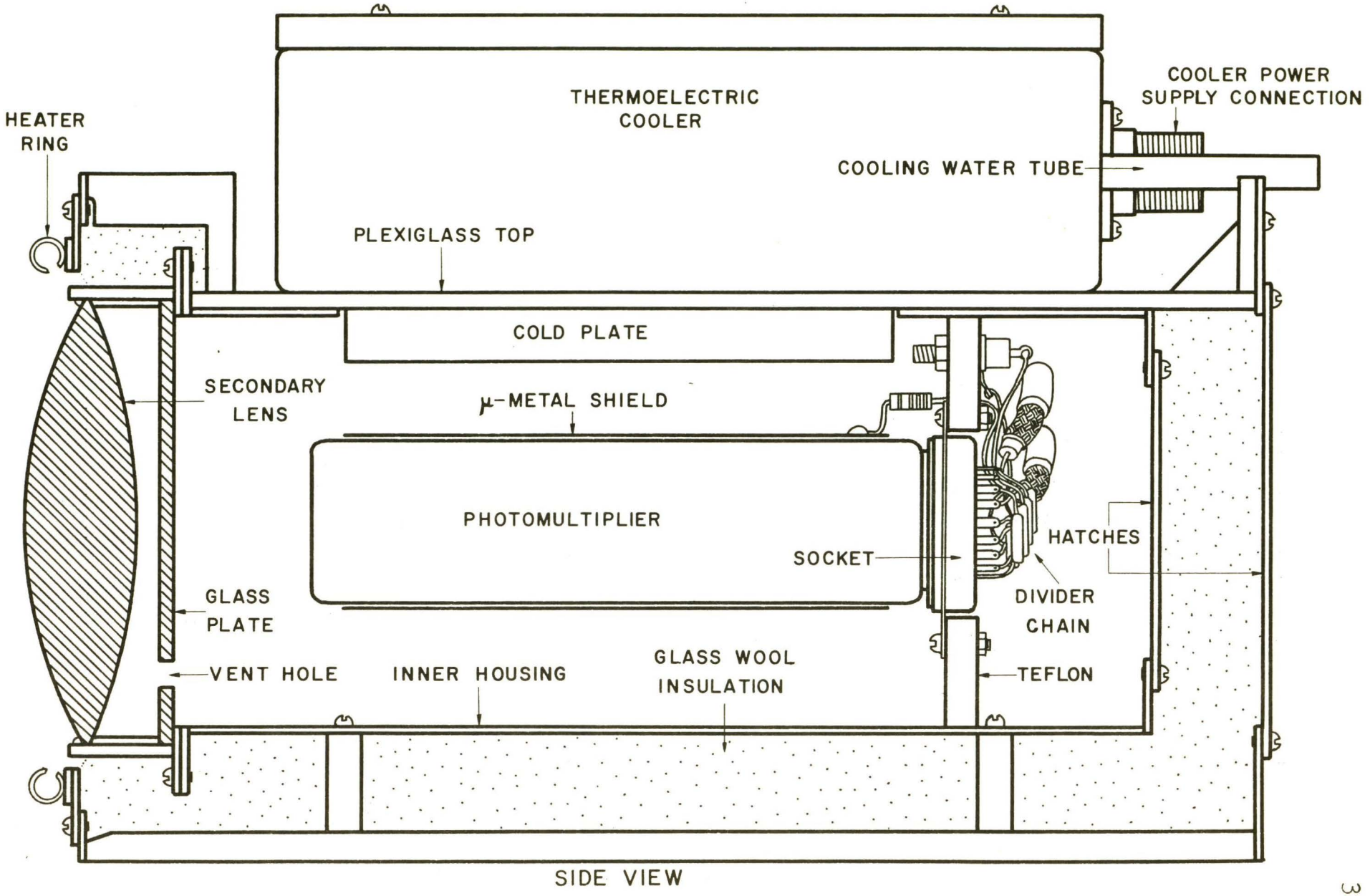

Figure 3.6.2
Inside view of cold box, full scale

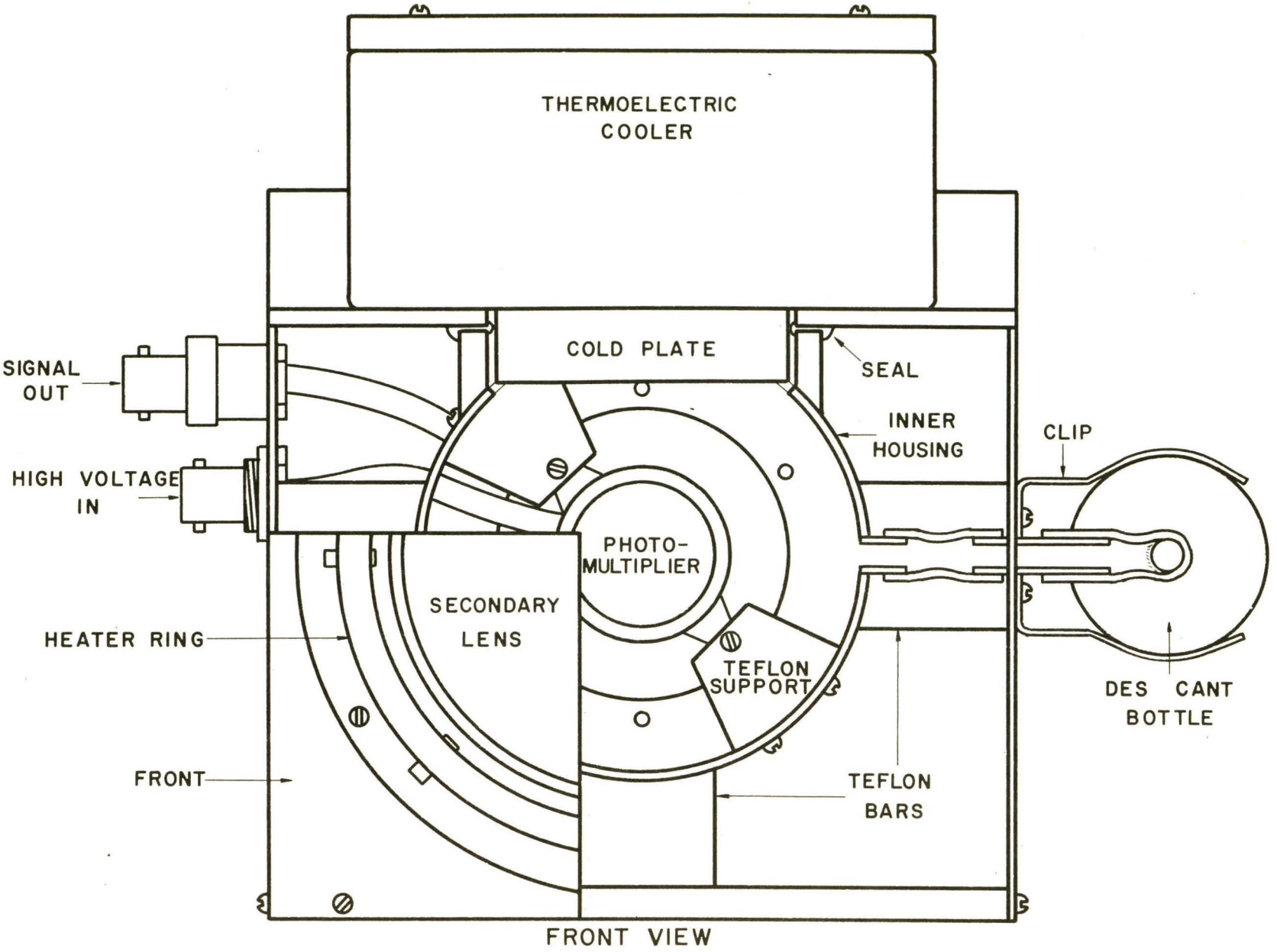

Figure 3.6.3
Cutaway view of cold box, full scale

through the calcium chloride desiccant. The original air is dehumidified by loosening the rear hatches and forcing air through the desiccator for several minutes.

The inner housing is supported by six teflon bars, and the entire space between it and the outer box is packed with glass wool. The box is held to the top of the baseplate by two screws in a slot, so that the beam may be properly focussed on the photocathode. Once focus is achieved, the screws are tightened and no further adjustment need be made.

3.7 Alignment and focussing.

A minimum of three hours is required for the thermoelectric cooler to reduce the temperature of the inner photomultiplier housing to -20° C. The valves on the cooling water tubes are first opened and the water is then turned on. The cooler power supply is then switched on and the thermostat is set to -20° C. Refrigeration of the photomultiplier significantly reduces dark current noise caused by the emission of thermal electrons from the photocathode and dynodes.

Next, the platform is moved down to the approximate pre-recorded zero-velocity position as indicated by the calibrated discs on the shaft of the screw. The mirror is attached with the four machine screws. Just before the screws are tightened, the base of the mirror holder is pulled parallel to the mirror, away from the platform. This ensures that the mirror is similarly positioned each time so as not

to cause a change of focus.

The grating is moved to the correct rotation, 323.0° being used for the masks described. Covers on the collimator, grating, and camera mirror are removed.

The emission lines of a mercury gas discharge tube are used for aligning the mask. The image slicer is used, with the mercury lamp resting immediately in front of the slicer opening. Vertical alignment is facilitated by clear slots left in either end of the mask. The platform is moved 15 mm. to the red, bringing two suitable lines into position in the slots. The vertical position of each line is viewed with a small first-surface mirror behind the mask, as in Figure 3.7.1.

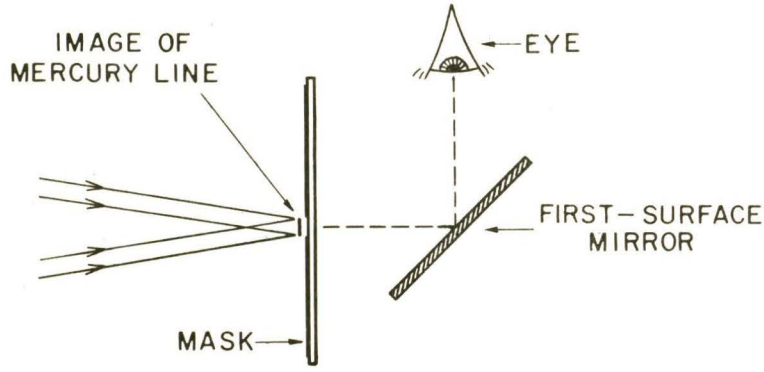

Figure 3.7.1

Vertical mask alignment.

The maskholder is loosened and the mask is nudged up or down until the line is centered vertically in the slot. This is performed for each end. The adjustment is awkward but can be done in a few minutes by an experienced operator.

The platform is now moved back to the zero-velocity position for focussing. The mask is focussed by means of a procedure called the Hartmann focus test. From the control room a diaphragm is rotated into place just behind the image slicer. Either the left or right half of the beam can be obstructed by rotating the control knob. Each half of the beam will of course produce a complete image of a mercury emission line, but the images will not be coincident upon the mask until focus is achieved. When the slow scanning mode is to be used, the test is begun by locating a mercury line near one end of the mask, as close to the edge of the artificial spectrogram as possible. The mask is then obscured with paper stops except for a narrow 1/4-inch region around the chosen line. The line is easily detected in the darkened Coudé room by holding a sheet of paper in front of the mask. The dust cap is removed from the secondary lens, and the amplification and time constant on the preamp are turned to their lowest values. For very slow scanning of the line, a thin glass plate on a slowly rotatable mounting is positioned in the beam behind the image slicer. The lights are turned off and the p.m. tube power supply is switched on; 600 volts is sufficient for the test. The emission line must now be made to coincide with an aperture in the mask, without moving the platform more than 1 mm. The output is monitored on the chart recorder while the platform is moved very slowly. When a suitable peak is recorded, the drive motor is switched off while the recorder pen is at the top of the peak. The thin

glass plate displaces the beam slowly by refraction through the glass. The rotation motor is operated until the pen has travelled down one side of the peak. As mentioned previously, two non-coincident peaks will be recorded from each half of the beam during scanning if the line being used is not in focus. The Hartmann diaphragm is brought into position, and the rotation motor is reversed. As the line is scanned, the diaphragm is moved from left to right every second or so. In this way both halves are scanned alternately and any displacement between the peaks is immediately obvious. If focussing is required, the p.m. tube power supply is switched off and the appropriate end of the mask is shifted in the direction of focus by the micrometer screw. The scanning is repeated and further focus adjustments are made until the peaks are coincident, as in Figure 3.7.2. The entire procedure is repeated for the other end of the mask. If any gross adjustment is made to the second end, the first end should be rechecked in case it has been affected.

The focussing procedure prior to operation in the rapid scanning mode is similar to that of the slow scanning mode, although the mercury lamp cannot be used due to the 120-cycle modulation of the light. The refracting plate drive motor is synchronous, causing integration of the 120-cycle signal in the analyzer. In order to avoid this signal, the comparison source lines are used, and the mask is partially obscured and adjusted as above. The output from the left and right sides of the beam is integrated for a

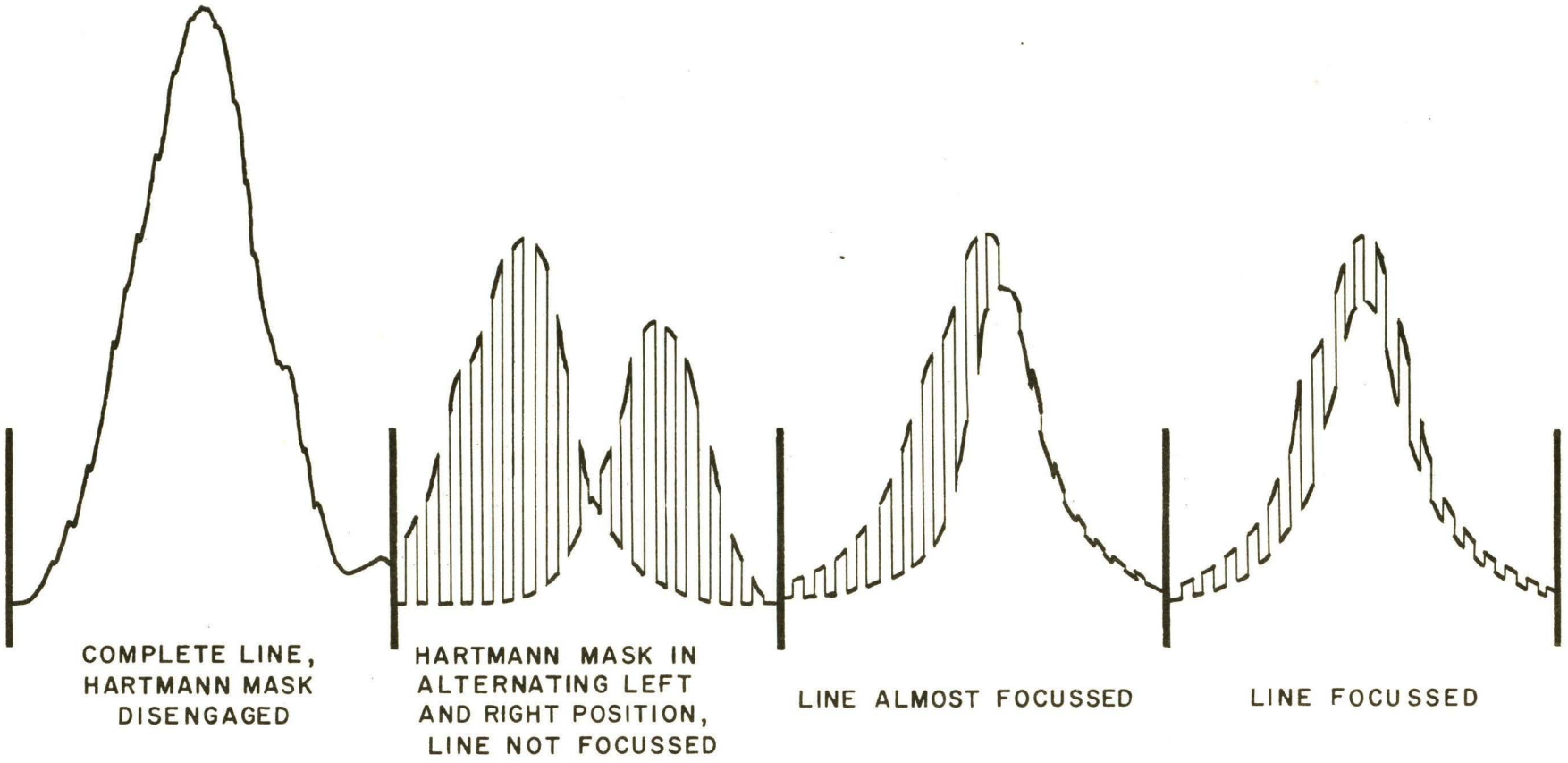

Figure 3.7.2

Typical slow scan output during Hartmann focus test

suitable length of time in different quarters of the analyzer memory. Both quarters may be displayed simultaneously on the oscilloscope, and any shift between the peaks is immediately obvious.

3.8 Operation

The procedures relevant to operating in the slow scanning mode will be discussed, followed by a discussion of operation in the rapid scanning mode.

At the commencement of a slow scan observing schedule, a scan of the comparison spectrum is executed to provide a reference peak on the chart recorder. In preparation for this, the image slicer is replaced by the slit and the slots at the end of the mask are blocked with paper stops. The prisms used to deflect the light from the comparison source are moved into position against the slit. Satisfactory preamp settings are X10 for the amplification and .01 for the time constant. Usually the chart recorder zero point requires adjustment also. A good peak is obtained at coincidence when the p.m. tube voltage is set to 600 or 700 volts, with the slit opened to 0.5 mm. The scanning rate chosen should be the same as the rate to be used for the stellar runs. A rate of 126 km./sec. per minute is used in the results presented. Five scans in the red direction and five in the blue are sufficient. This is repeated at the end of an observing run to check for instrumental drift.

Scans of stellar sources can now be made. The

telescope is set on the star and the image is moved into position on the slit as seen through the slit viewer. Settings of the slit, preamp, monitor channel, and power supply voltages are described in Chapter 4. The exposure meter power supply must now be turned on so that the ratio technique may be used. Care must be taken that the p.m. tube and electronics are allowed to stabilize. Otherwise, annoying zero-point adjustments may be necessary part way through a run.

During the comparison scans the downward reference spikes should be clearly coded. This labeling must be continued throughout the stellar runs so that when the data is to be reduced, the operator knows where the stellar dip occurred relative to the comparison peak.

When the run is complete, the scans are repeated for the next star to be observed. Adjustments to the p.m. tube voltage and monitor channel controls may be necessary if the magnitude of a star is appreciably different from the previous one observed. At the end of an observing schedule the comparison scans are repeated.

At the beginning of operation in the rapid scan mode, single scan recordings of the photomultiplier dark current for a 1000 volt supply voltage will indicate that the system is functioning normally. Light from the comparison source is made to pass through the image slicer, and the spectrometer platform is moved very slowly until the comparison peak occurs in the center of a scan as seen on

the oscilloscope. The data is erased and a new peak is recorded in one quarter of the analyzer memory for later use as the reference peak.

The image slicer may also be used for the stellar scans, as the fluctuations produced by non-even illumination of the slices are of a longer period than the scanning time. The ratio technique is not used, as the atmospheric effects are also not resolved at this scanning rate.

The telescope is now sighted on a star and the image is moved into position on the slicer entrance slot as seen through the slicer viewer. The analyzer is set for the number of scans to be integrated, and to the desired time constant. If a well-defined dip does not appear to be forming after half the scanning time is over, the number of scans can be doubled. For the stars examined in Chapter 4, the time constant is set at 10 milliseconds. The completion of 512 scans requires 8 minutes and 32 seconds per star. During this time the operator may set the telescope preselector to the coordinates of the next star to be observed.

At the completion of the scans the data is plotted on the same graph as the comparison peak by an x-y recorder for later processing. Plotting the negative of the comparison peak causes both dips to occur in the same direction on the paper.

The next star may then be centered and measured. At least two more comparison peaks should be recorded during the night to check for instrumental drift.

CHAPTER 4

REDUCTION OF DATA AND PRELIMINARY RESULTS

4.1 Reduction

Reduction of the slow scan data is simply a matter of measuring the displacement between the comparison peaks and stellar dips with a ruler. Factors dependent upon the scanning rate and chart paper speed are then applied to deduce the radial velocity.

A typical comparison and stellar slow scan record is shown in figure 4.1.1. For each star, five scans were made in the direction of red shift and five in the direction of blue shift. Settings are described in Table 4.2.1. A chart paper speed of 25.4 mm. per minute was used, with a scanning rate of 126.2 km./sec. per minute. Thus 1.0 mm. on the chart paper corresponded to 4.97 km./sec.

The dips were bisected on the chart and a weighted average of the five blue dip positions and then of the five red dip positions was taken. These average positions were compared with the averages of the blue and red comparison peak positions, respectively, to obtain the displacement. The two values from the red and blue scans were then averaged to eliminate the effects of instrument backlash and time constant. The difference between the experimental results and the values given in the General Catalogue of Stellar Radial Velocities of Wilson (1953) was found for each star, and these differences were averaged with equal

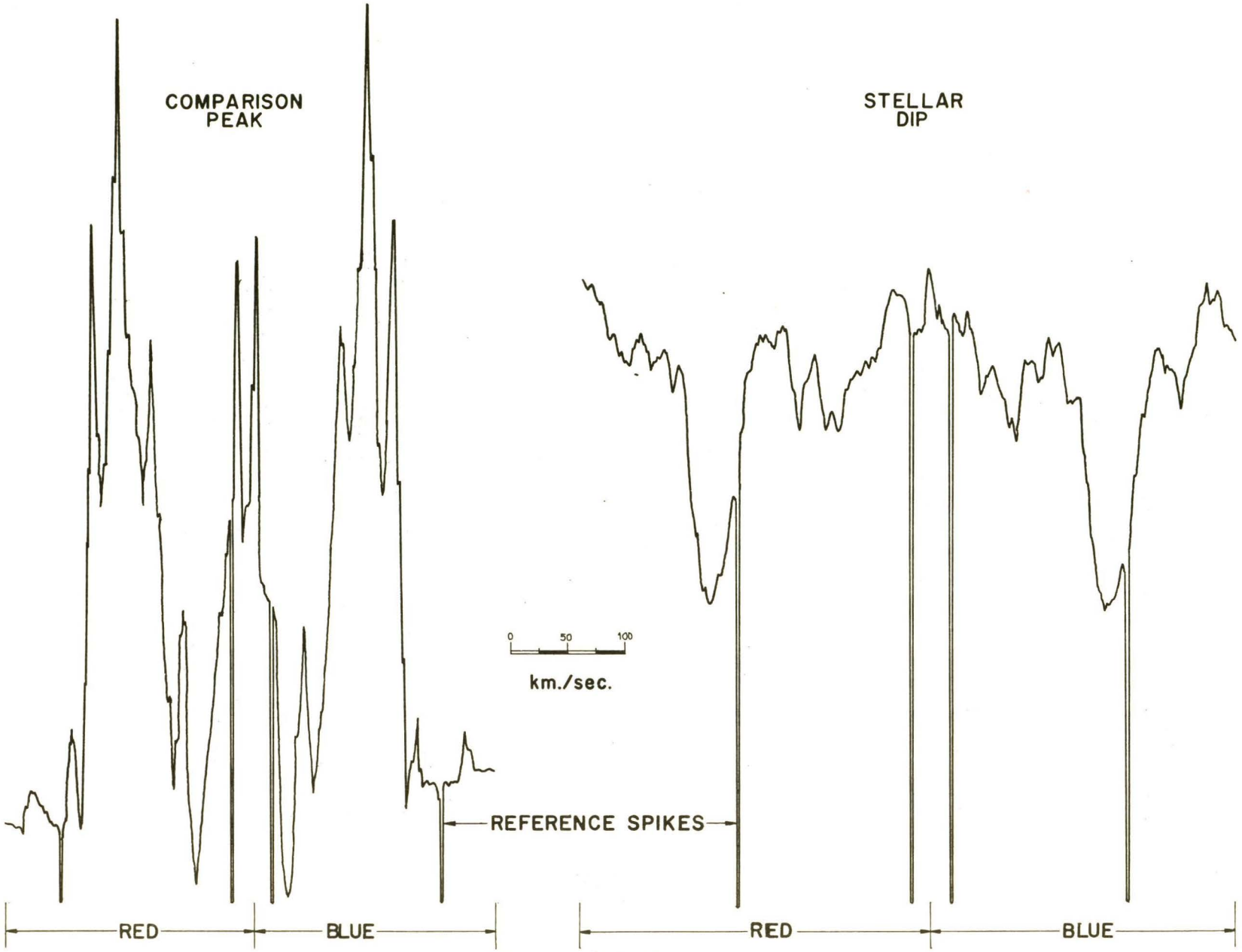

Figure 4.1.1
Slow scan output from strip-chart recorder

weight to obtain the instrumental correction. The instrumental correction was a consequence of the non-correspondence of the comparison peak with the zero-velocity position. In this case the correction was found to be +12.2 km./sec. The same correction was applied to each star. There is no reason to suppose that the correction will vary significantly from night to night, but this has not yet been investigated. The establishment of a constant correction after many observations will eliminate the need to include reference stars of known velocity in an observing program.

The reduction of rapid scan data is similar to slow scan data reduction, although as mentioned in Section 3.4, the displacement as printed by the analyzer is not linearly related to the Doppler shift. A typical example of the analyzer printout is shown in Figure 4.1.2. The address number, in which output is stored in the analyzer, is a linear function of the incidence angle of the beam on the refracting plate. However, the beam displacement is a markedly non-linear function of the incidence angle, since the beam encounters the refracting plate at angles up to 45° on either side of normal incidence.

The function was found by scanning the comparison spectrum at different positions of the mask. The mask position was read from the calibrated drum on the slow scanner screw, and the corresponding address was found from the digital readout facility of the analyzer. A least

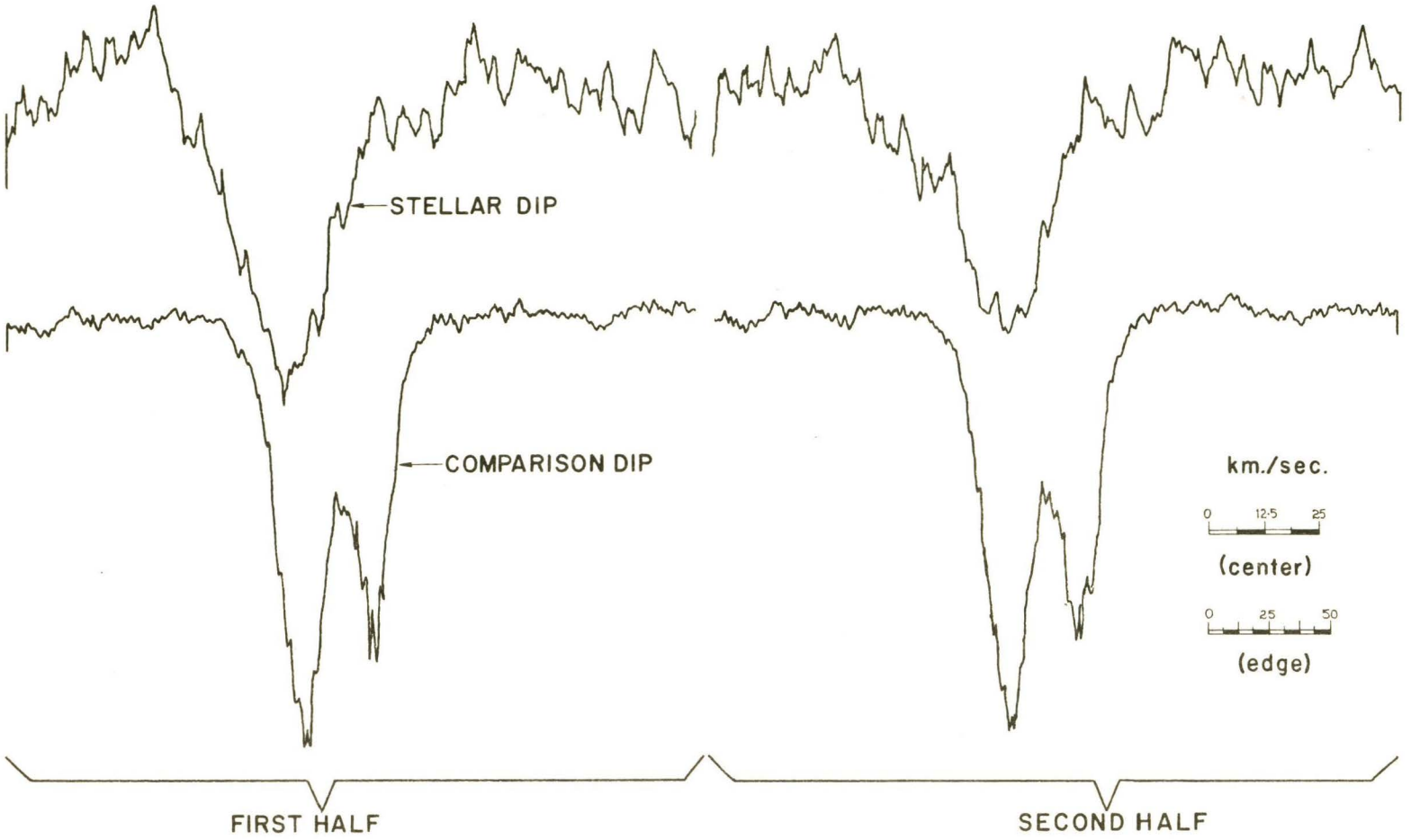

Figure 4.1.2

Rapid scan output from analyzer

squares fit of a cubic polynomial was made to 100 such measurements, yielding the relation:

Position (mm.) = $K + 3.50 \times 10^{-3} A - 6.17 \times 10^{-6} A^2 + 8.10 \times 10^{-9} A^3$,

where A is the address number. Relative, not absolute, positions of dips were relevant; therefore K was arbitrary.

Each rotation of the refracting plate yielded two scans which were recorded separately and were displayed side by side on the oscilloscope. The first scan occupied channels 0 to 514, and the second occupied channels 515 to 1023. The velocity range of a scan was about 180 km./sec. The total width of each scan, the center of the comparison dip, and the center of the stellar dip were all measured on the paper with a ruler. The dip position was converted into address number, which was in turn converted into position by the above function. Subtraction yielded the Doppler shifts. The rVs factor was then applied to obtain the velocities. Each of the two scans per star was processed independently to obtain a measure of the reliability of a single record. The average difference between pairs was 1.0 km./sec.

Again, a comparison of experimental and Catalogue velocities was made, and the differences yielded an instrumental correction of +15.5 km./sec.

Instrument settings and results are presented in Table 4.2.2.

4.2 Results

Slow scan settings and velocities for seven stars observed are given in Table 4.2.1. Settings and velocities for seven rapidly scanned stars are presented in Table 4.2.2.

The residuals, or difference from the Catalogue value, have been plotted against spectral class and magnitude in Figure 4.2.1. It appeared that the residuals were independent of both spectral class and magnitude.

The standard deviation in velocity, or root mean square residual, for Table 4.2.1. was 2.25 km./sec., and for Table 4.2.2 was 2.75 km./sec.

All stars: Projected slit width = 130μ

Preamp setting: X 100, .10

Mask rVs = 156.5 km./sec./mm.

R.M.S. residual = 2.25 km./sec.

Star	ϵ Tau	ϵ Leo	5 Cvn	6 Cvn	HR 4783	27 Com	o UMa
Magnitude	3.54	2.99	4.77	5.02	5.43	5.12	3.37
Spectral class	K0 III	G0 II	G7 III	G8 III	K0 III	K3 III	G5 III
P.M. tube voltage	800	900	900	900	900	900	800
Monitor voltage	860	1000	1100	1100	1100	1100	900
Displacement from iron							
Blue runs (mm.)	+8.65	-3.60	-9.61	-8.41	-10.61	+1.88	+2.26
σ (mm.)	.24	.55	.73	.84	.50	.73	.51
Red runs (mm.)	+14.30	+3.45	-2.98	-2.72	-5.72	+8.71	+8.53
σ (mm.)	.62	.30	.55	.82	.65	.70	.20
Average	+11.47	-.08	-6.30	-5.57	-8.19	+5.30	+5.40
Uncorrected velocity	+57.0	-0.4	-31.3	-27.2	-40.7	+26.3	+26.8
Corrected to Sun + inst. correction	+41.5	+6.0	-16.2	-7.2	-18.3	+54.1	+20.1
Catalogue	+38.6	+5.0	-13.1	-3.5	-19.8	+53.0	+19.8
Residual	-2.9	-1.0	+3.1	+3.7	-1.5	-1.1	-0.3

Table 4.2.1

All stars: Projected slit width = 16 μ

10 millisec. time constant

Mask rVs = 158.7 km./sec./mm.

R.M.S. residual = 2.75 km./sec.

Catalogue number of star	6476	6570	7254	8688	9554	10069	10570
Magnitude	6.0	6.5	7.1	7.0	7.4	7.8	7.4
Spectral class	gK2	K0	gK3	gG5	gM3	dK6	dG3
P.M. tube voltage	1000	1000	1000	1200	1200	1200	1200
Scans	256	512	512	512	512	512	512
Displacement from iron							
Left (mm.)	+.2967	+.0168	-.1140	-.0800	-.4866	-.3554	-.1205
Right (mm.)	+.2934	+.0049	-.1111	-.0773	-.4750	-.3638	-.1159
Uncorrected velocity							
Left	+47.09	+2.67	-18.09	-12.70	-77.22	-56.40	-19.12
Right	+46.56	+0.78	-17.63	-12.27	-75.38	-57.74	-18.39
Average corrected to Sun + inst. correction	+34.3	-7.6	-11.5	-15.9	-55.7	-23.6	-2.3
Catalogue	+33.9	-4.1	-12.0	-18.0	-52.0	-28.3	-1.8
Residual	-0.4	+3.5	-0.5	-2.1	+3.7	-4.7	+0.5

Table 4.2.2

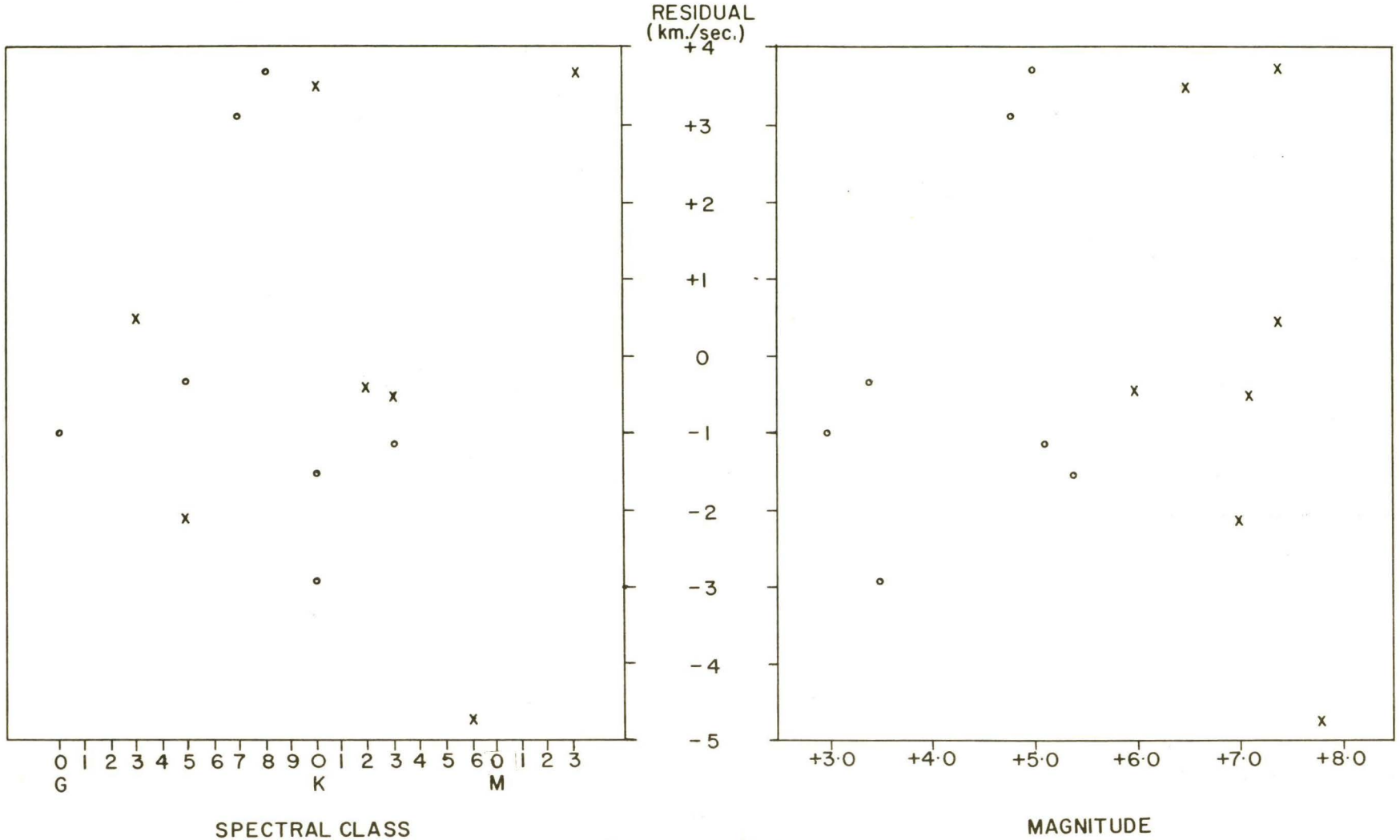

Figure 4.2.1

Graphs of spectral class and magnitude versus residuals

CHAPTER 5

DISCUSSION AND CONCLUSIONS

The greatest uncertainty in velocity from slow scan data arises from degradation of the dip by variations in atmospheric extinction with a period of the order of a few seconds. At the large time constant used, the noise from the photomultiplier and amplifier is not troublesome. Owing to the Victoria climate, any given observing schedule is likely to be conducted under a non-photometric sky; hence, the ratio technique must be used and care must be taken to optimize amplifier settings. Recordings of signal while the spectrum is not being scanned have indicated that there is much room for improving the ratio compensation of light fluctuation.

These fluctuations are not resolved by rapid scanning; however, significant noise of another nature is present. At high rates of scan, the time constant used must of necessity be small to avoid distorting the dip, and so the output from individual photo-events is resolved and recorded. It is only by integration of a few hundred scans that a distinction between random output and the periodic dip can be made, as the signal/noise ratio increases as the root of the number of scans. Photomultiplier dark current and, to a lesser extent, short period light fluctuations are now the significant contributors of noise. Most dark current output

pulses originate by random emission of electrons at various stages along the multiplier dynode chain, and hence are of smaller amplitude than pulses from photo-events. Their numbers increase rapidly with decreasing amplitude, and at low light levels the contribution to the total current is significant. This contribution can be effectively attenuated by a pulse-height discriminator of the type used in pulse-counting equipment. A slower scanning rate, perhaps one-tenth of that used previously,would allow a longer time constant to be used in smoothing the resolved input. A short time constant ratio amplifier would take care of any atmospheric fluctuations.

The accuracies of the two scanning methods seem similar, but it must be remembered that the rapid scan velocities represent stars of an average of 2.7 magnitudes fainter than the slowly scanned stars. The scanning time is less than one-half of the slow scan time per star, and data redudtion is much simplified. The improved sensitivity is for the most part probably a result of the greater discrimination employed when choosing lines for the second mask.

Future modifications made to the spectrometer to increase the accuracy and limiting magnitude will undoubtedly follow the rapid scan line of development. It offers reduced observing time per star, ease of focussing, and all the advantages of digitally-stored computer-compatible data.

The chief limitation of photoelectric radial velocity measurements is the dependence on the coincidence of a well-defined spectrum with similar mask. This limits the instrument to the measurement of sharp-lined stars in the spectral classes from F to M. The lines of early-type stars are broad and few in number; at best, a shallow dip would be recorded, but the accuracy could not compete with the photographic method. The profusion of lines in late-type stars would cause many pseudo-coincidences of sufficient strength to cause ambiguities.

The second mask appeared to perform equally well over the range from G3 to M3. Performance at either end of the range from F to M could be optimized by producing several masks, each covering a portion of the range. The changing and refocussing of a mask can be done in thirty minutes.

A few fundamental instrumental accuracy limitations are worthy of consideration. As mentioned in Section 3.1, the mismatch at either end of the plate is small in comparison with the half-width of the dip, and is of opposite sign at opposite ends of the mask.

Another error may arise from variations in spectral energy distribution, which changes the effective rVs factor of the mask. Griffin (1967) has found that G5 dwarfs and early M giants may have effective wavelengths differing by ± 15 Å from a K2 spectrum, as seen through his mask. The same difference would change the rVs factor of the K2 III

mask by ± 0.53 km./sec./mm. In other words, the velocity of a 100 km./sec. star could be in error by ± 0.33 km./sec. for this reason. The lack of correlation between velocity residuals and spectral class in Figure 4.2.1 indicates that there is no means of accounting for the dependence of effective wavelength on the spectral class of the star.

The smallest detail that can be resolved in the output is limited by the width of one channel in the analyzer. When the beam is near normal incidence on the rotating refractor plate, the channel width is 0.31 km./sec. For large angles of incidence at both extremes of the scanning range, the width is 0.56 km./sec. Any smaller detail is lost. However, widths of this size are only about one per cent of the half-width of a dip.

A combination of the above effects imposes a limit of up to 0.9 km./sec. on the velocity accuracy of a 100 km./sec. star.

Finally, one must investigate the merit of the General Catalogue of Stellar Radial Velocities. The stars observed, with the exception of ϵ Tau, ϵ Leo, and o UMa, were all listed as having "b" quality velocities, meaning that the standard deviation per star is between 1.4 and 3.0 km./sec. The usefulness of the Catalogue as a means of measuring the accuracy of the spectrometer is thus somewhat limited.

APPENDIX A

48-INCH TELESCOPE AND 9682 SPECTROGRAPH

The main features of the 48-inch telescope and spectrograph are depicted in Figure A.1. The primary focal ratio of f/4 is changed to f/145 at the secondary mirror. After two more reflections which send the beam down the polar axis to the floor below, a combination of totally-reflecting prism and lens diverts the beam toward the slit and changes the focal ratio to f/30. Each of the three mirrors following the primary is mounted on a rotatable turret with two others, so that mirrors may be chosen for high reflectance in the blue or red region.

After passing through the slit or image slicer, the light enters the Coudé room. The slit is basically two polished metal jaws forming a variable vertical slit at the Coudé focus of the telescope. The projected slit width at the spectrograph focus is about one-third the slit opening. The image slicer is a refinement of a slit and decreases the length of an exposure when the size of a stellar image is greater than the width of a slit. The slicer is used in alignment procedures since it gives mercury lines of the proper length for vertical alignment of the mask. However, it is rejected in favour of the variable slit for stellar slow scans, as the image slicer slit width is not controllable. Uneven illumination of the slices can also be a serious source of noise when slow-scanning. A complete

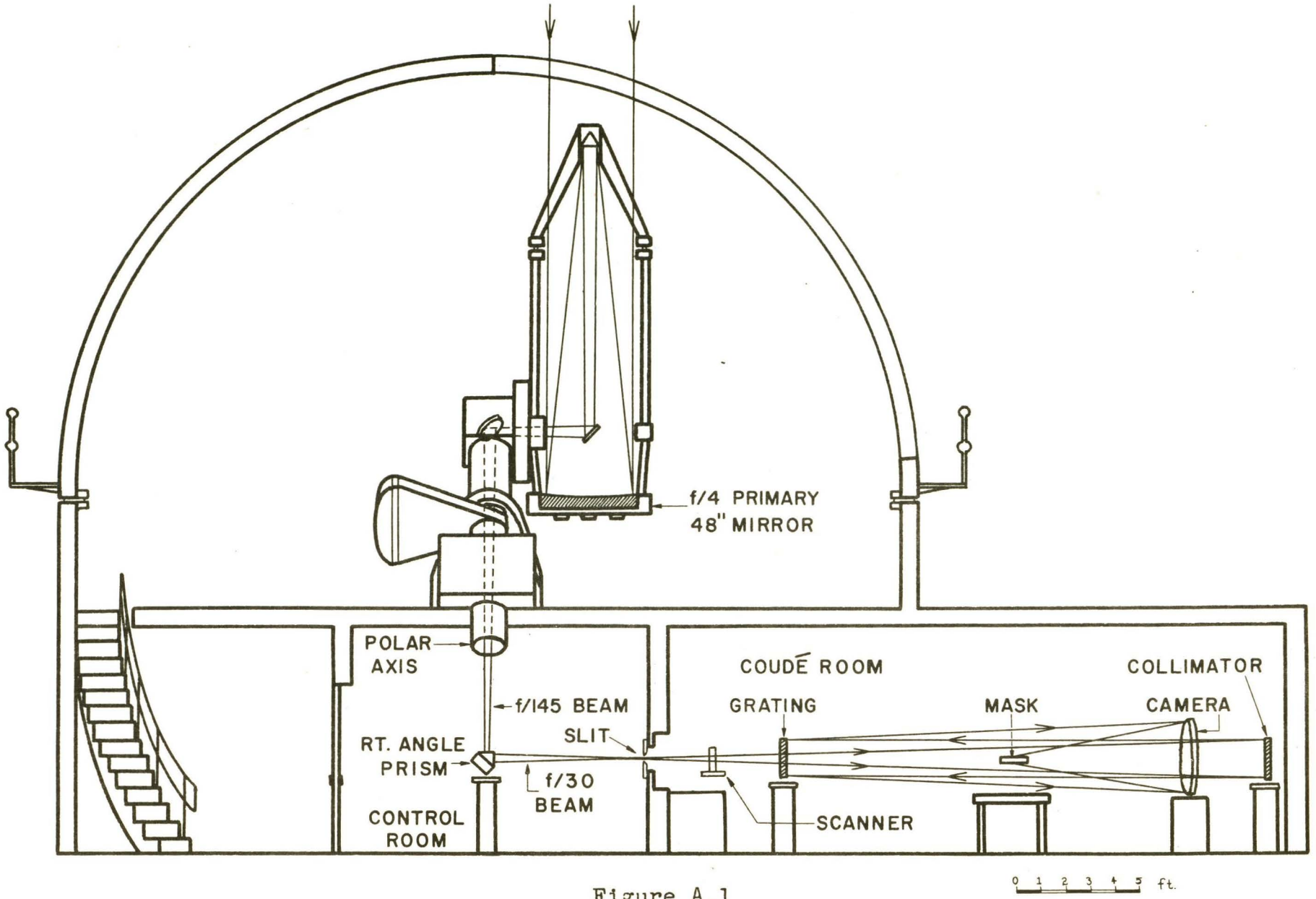

Figure A.1

The 48-inch telescope and 9682 spectrograph

description of the optics of the image slicer has been published by E.H. Richardson (1968).

Figure A.2 shows the layout of the 9682 spectrograph in the Coudé room. The room also contains a 32-inch focal length camera which is not shown. The grating is a mosaic of four 6 by 7 inch replica gratings with 830.77 grooves per mm., blazed for the second order blue. Combined with the 96-inch focal length camera mirror, it has a reciprocal dispersion of about 2.4 Å/mm. The photographic plateholder is removed for R.V.S. operation. In the figure the beam appears to coincide with the position of the large flat. The beam is not obstructed by the flat, however, due to selective illumination of the light slices, as explained in Section 3.2. All elements are easily accessible as they are horizontally arranged about 4 feet above the floor. The entire floor is isolated from the walls and forms a stable optical table free from flexure.

Details of the immediate pre-slit optics in the control room are also shown.

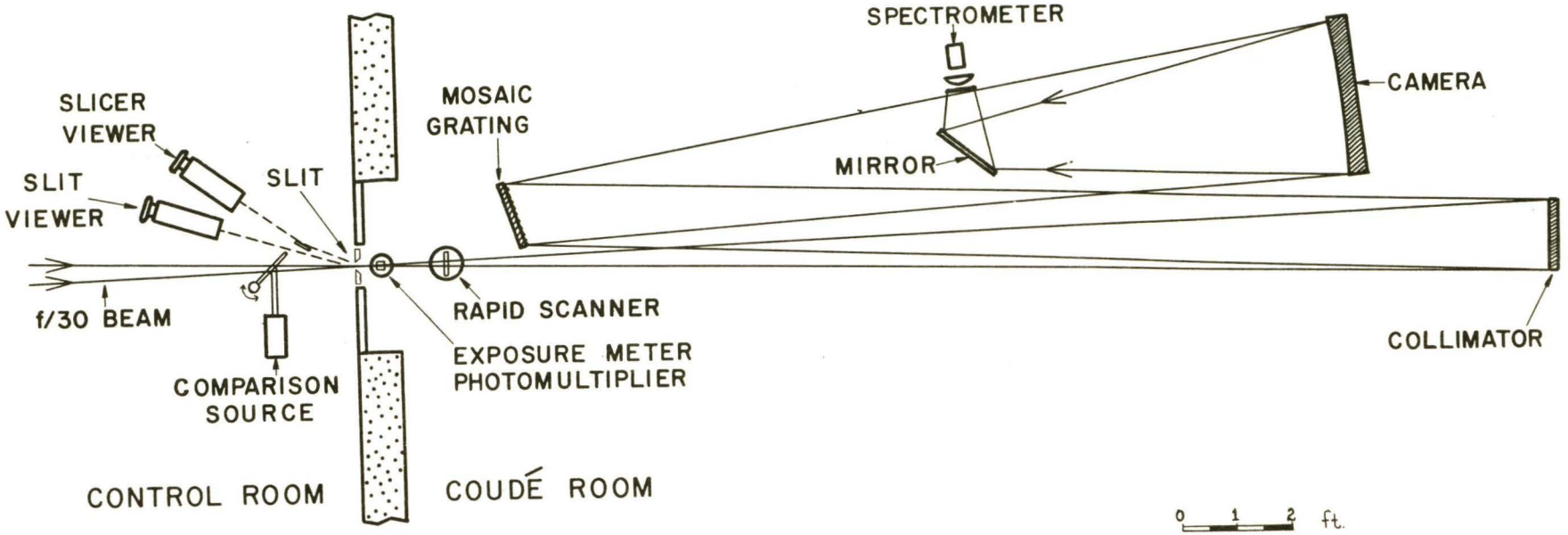

TOP VIEW

Figure A.2

The 9682 spectrograph

APPENDIX B

PRODUCTION OF THE ARTIFICIAL MASK

It was previously mentioned that the unaltered spectrogram of the sky was found to be unsuitable for use as a mask. The chief causes were the high transmission and the spillage of light above and below the exposed portion. Subsequently the production of an artificial mask was undertaken and an acceptable one was produced on the first attempt. The problem was to build a machine for making an artificial spectrogram in which lines and line widths could be reproduced on a standard 2 by 8 inch plate, preserving the relative positions of the chosen lines.

The mask machine described below is illustrated in Figure B.1.

The original sky spectrogram was clamped to the stage of the travelling microscope, and an unexposed plate was clamped to the plateholder. Lines of the proper vertical length and spacing were projected from a three-slit source onto the plate through a 25 mm. focal length eyepiece. Each line to be reproduced was centered on the microscope crossline and a key for either a stellar line or a comparison line was then pressed. The exposure time for a IV-0 plate was four seconds per line. The projected slit width was 30μ. Wider lines required multiple overlapping exposures, the largest being 120μ. As the plate and sky spectrogram were

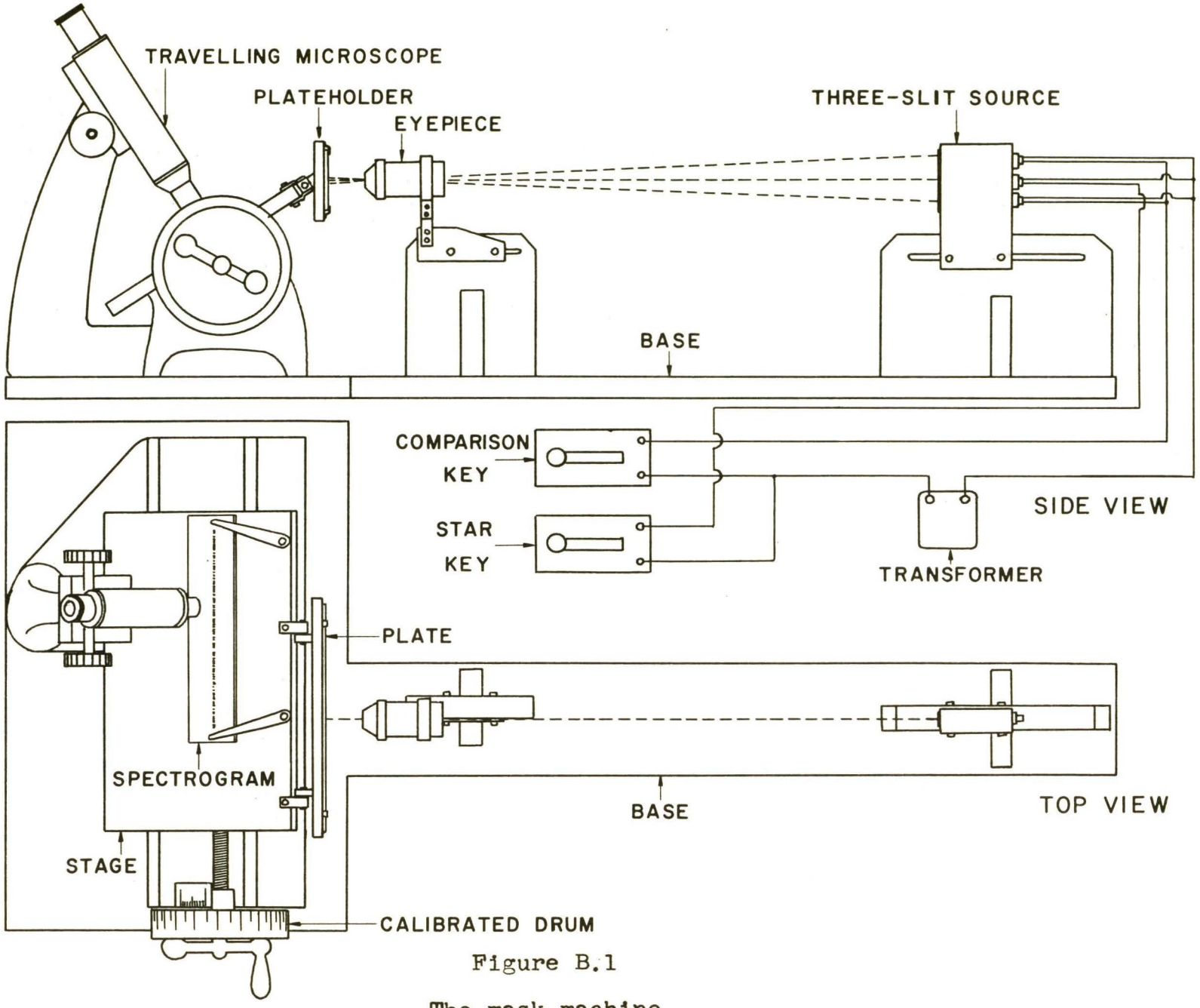

Figure B.1

The mask machine

both held fast to the travelling stage, the relative spacing of all the lines was preserved. The developed plate resembled a negative of an emission-line spectrum. The mask was made from a contact print of this plate, thus leaving an aperture corresponding to each reproduced line.

A great deal of trouble was originally encountered in reducing the projected slit width to 30 μ. Light scattering inside the eyepiece produced a dark halo about 140 μ wide around the central 30 μ core. It was finally eliminated by a cardboard plate with a 1.0 mm. slit attached to the source side of the eyepiece tube. Then, 25 line pairs per millimeter were easily produced with no overlapping.

The components were held rigidly to a 3/4-inch thick plywood base. Extensive use was made of cardboard shielding around the plate to prevent scattered light from clouding the plate. The G2 V mask was produced in a darkroom and required two hours at the microscope.

An improved K2 III mask was produced by first choosing lines from a photometric atlas of the spectrum of Arcturus by R.F. Griffin (1968). Only well-defined lines having a residual intensity of less than 30 per cent of the continuum were reproduced. Instead of sighting on lines in the stellar spectrogram, the wavelengths as taken from the atlas were converted into plate position by the relation:

$$\text{Scale position in mm.} = A + .00005916\,(A - 76.5)^2 - .030,$$

where $A = \lambda(\text{Å})/2.3755 - 1838.584$.

This equation was derived by trial and error fitting of a curve to twenty-one iron lines of known scale position and wavelength. It was accurate to .003 mm.

The wavelengths of 247 lines were converted to scale positions and then the calibrated drum of the travelling microscope was moved to each, all lines being exposed in accordance with the schedule. The basic line width was 40μ.

A study of the convolution of a rectangle and a Gaussian function was made to determine the optimum width of the mask apertures. A cutout in cardboard of a rectangular aperture was moved across a cutout of a Gaussian aperture, and the amount of light transmitted by the cutouts was monitored by a photoresistive cell. This simple device worked very well, and plots of the transmittance were made for several rectangle widths. The width of the Gaussian at half-maximum is called the half-width. It was found that the convolution depth ceased to increase significantly when the rectangle width exceeded about 1.1 times the Gaussian half-width, as seen in Figure B.2. A further increase resulted only in a rapid increase of the half-width of the convolution, and so the optimum aperture width was estimated to be 1.1 times the spectral line half-width as measured in the photometric atlas. The line profiles of typical lines chosen from the atlas were approximated well enough by a Gaussian to make the convolution study meaningful.

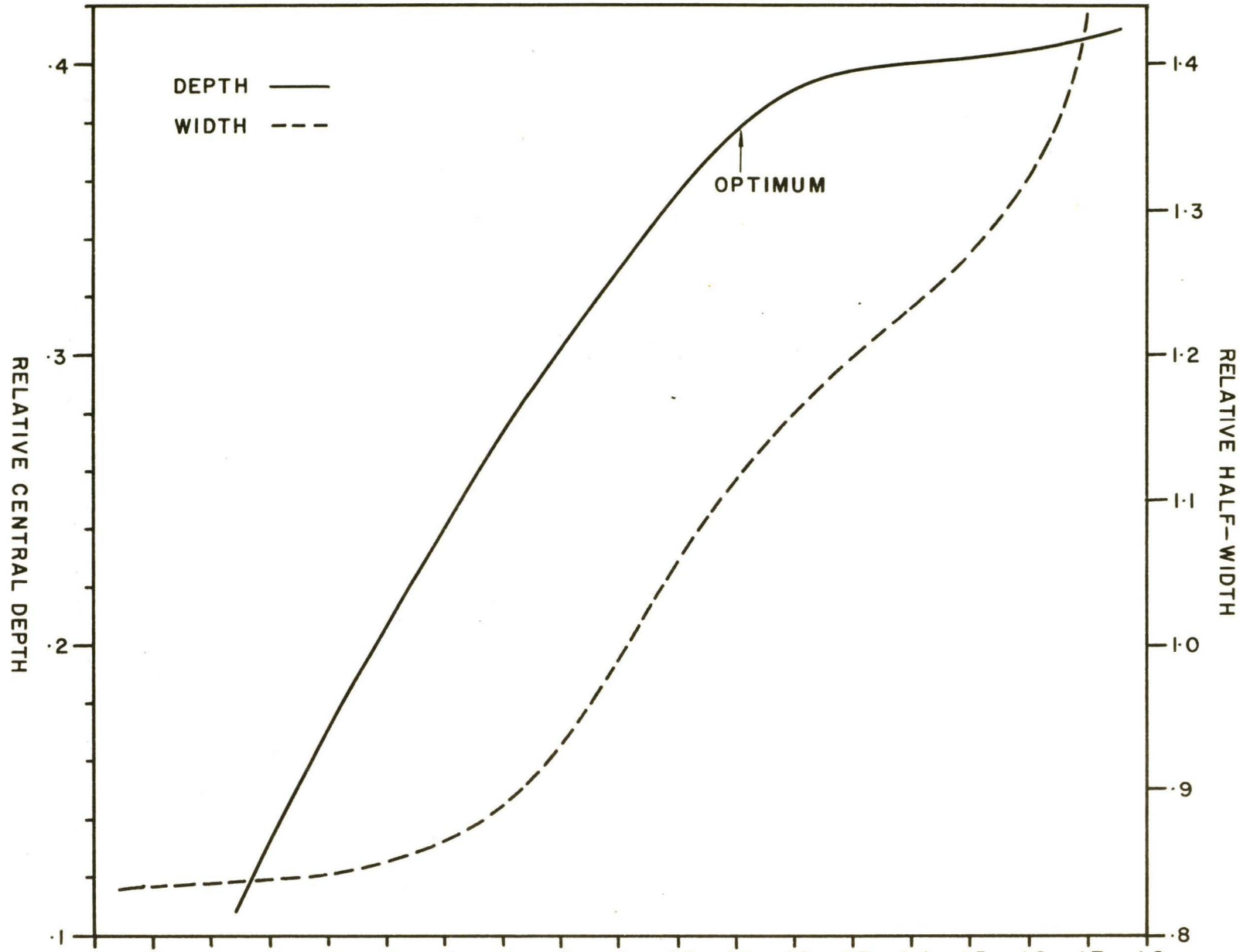
DEPTH
WIDTH
OPTIMUM
RELATIVE CENTRAL DEPTH
RELATIVE HALF-WIDTH
RECTANGLE WIDTH / GAUSSIAN HALF-WIDTH
·4
·3
·2
·1
1·4
1·3
1·2
1·1
1·0
·9
·8
0
·1
·2
·3
·4
·5
·6
·7
·8
·9
1·0
1·1
1·2
1·3
1·4
1·5
1·6
1·7
1·8

Figure B.2

APPENDIX C

MAINTENANCE INSTRUCTIONS

Several parts of the instrument must be routinely serviced. First of all, the calcium chloride desiccant must not be allowed to saturate with moisture. The desiccator is recharged by removing it from the clip on the cold box, removing the vented stopper, and pouring the desiccant out. It may be refilled with new dry crystals, or the old ones may be dried out by heating at 300° F. for one-half hour in an oven. Care must be taken to insure that the perforated cardboard screen is in place at the bottom of the desiccator so that the crystals cannot fall into the photomultiplier box.

The wide tracks of the scanner base should each be oiled with a few drops of light lubricating oil prior to each observing run. Pushing the platform back and forth a few times will spread the oil evenly.

The wheels of the movable support must also be oiled in addition to the mask focussing micrometer screws. This is mainly for rust prevention, hence the oil should frequently be swabbed over the wheel surfaces and micrometer barrels. Any excess must be wiped off completely, including excess oil from the tracks.

The Coudé room is quite dust-free, and so dusting of the optical parts is unnecessary. If it is ever required, a freon-jet duster should be used. Any smudges on the optics

can be wiped off with a clean tissue or lens cloth. A cap should be kept over the secondary lens during non-operation to prevent the photomultiplier from being exposed to the room lights.

If internal changes are required, the inner housing may be opened by removing the two rear hatches or the top of the cold box. When replacing the top, heavy grease or caulking compound must be spread thinly around the seal. The high voltage connection to the cold box should be removed before the box is opened.

REFERENCES

Griffin, R.F. 1967. Astrophysical Journal 148, 465.

Griffin, R.F. 1968. A Photometric Atlas of the Spectrum of Arcturus. Cambridge Philosophical Society. University Printing House, Cambridge.

Petrie, R.M. 1962. Astronomical Techniques, 63-81. Edited by W.A. Hiltner. University of Chicago Press.

Richardson, E.H. 1968. Journal of the Royal Astronomical Society of Canada 62, 313.

Wilson, R.E. 1953. General Catalogue of Stellar Radial Velocities. Carnegie Institute of Washington Publication 601. Kirby Lithograph Co., Washington.

Surname: STILBORN Given Names: JAMES RICHARD

Place of Birth: BRANDON, MANITOBA

Date of Birth: APRIL 27, 1946

Educational Institutions Attended, with Dates of Entering and Leaving:

UNITED COLLEGE (WINNIPEG)	1963 to 1965
UNIVERSITY OF MANITOBA	1965 to 1968
UNIVERSITY OF VICTORIA	1968 to 1970

Degrees, Diplomas, Etc., Awarded, with Dates and Names of Institutions:

B.Sc.(Honours)	1968	UNIVERSITY OF MANITOBA

Honours and Awards:

University of Victoria Graduate Fellowship, 1968/69 and 1969/70

THE UNIVERSITY OF VICTORIA LIBRARY

MANUSCRIPT THESIS

AUTHORITY TO DISTRIBUTE

AUTHOR: This thesis may be lent or microfilm copies made available:

(a) Without restriction [redacted]

(b) With the restriction that, for a period of five years (until _____) the written approval of the following is required:

(1) The Dean, Faculty of Graduate Studies .....

(2) The Author .....

(3) both the Dean, Faculty of Graduate Studies, and the Author .....

BORROWERS: The borrower undertakes, by signing below, to give proper credit for any use made of the thesis, and to obtain the consent of the author if it is proposed to make extensive quotations, or to reproduce the thesis in whole or in part.

Signature of Borrower	Address	Date